

# **MODELING OF LOCAL DAMAGE IN AUTOMOBILE INTERNAL COMBUSTION ENGINES**

**OLEKSANDR KRAVCHENKO  
ALEXANDER KHRULEV  
JURAJ GERLICI  
OLEKSII SARAIEV**



**ŽILINSKÁ UNIVERZITA  
V ŽILINE**

**Olexander Kravchenko, Alexander Khrulev,  
Juraj Gerlici, Oleksii Saraiev**

**MODELING OF LOCAL DAMAGE  
IN AUTOMOBILE INTERNAL COMBUSTION ENGINES**

Žilinská univerzita v Žiline  
EDIS-vydavateľstvo UNIZA  
2025

**Abstract.** The monograph examines a number of previously unnoticed and insufficiently studied mechanisms for the development of faults that cause local operational damage in automobile internal combustion engines. The general concept of modeling the processes and mechanisms of the occurrence and development of engine malfunctions is presented. The role, capabilities, purpose and features of mathematical modeling of processes that lead to damage and failure of engines are determined. The difference between modeling operational engine damage and modeling during design and research work is shown. The main processes of occurrence of local damage in engines are considered, mathematical models of the processes under consideration are described in detail, and modeling results are given using examples of specific structures. Experimentally, using the example of a specific automobile transport enterprise, malfunctions in the performance of car engines were identified during the warranty and post-warranty periods of operation; patterns of malfunction of units and parts have been determined. The issues of the need to store engine spare parts at a car service enterprise are considered, and the wear of engine interfaces is assessed. Based on the results of the research, it was noted that the developed models can be used in practice in determining the causes of malfunctions of engines of various types, and their use in expert studies can increase the accuracy and objectivity of expert opinions. The book is intended for undergraduate, graduate and postgraduate students as well as researchers majoring in Automobile operation, but may also be useful to engineers, experts and scientists in other fields related to the process research, design and operation of internal combustion engines.

Scientific redactor prof. Ing. Alžbeta Sapietová, PhD  
Reviewers prof. Dr. Sc. Tech. Alexander V. Belogub  
prof. Dr. Sc. Tech. Roman A. Varbanets

©University of Žilina, EDIS-Publishing House UNIZA  
Oleksandr Kravchenko, Alexander Khrulev, Juraj Gerlici, Oleksii Saraiev, 2025  
ISBN 978-80-554-2239-8

**CONTENTS**

<b>LIST OF SYMBOLS</b>	<b>5</b>
<b>PREFACE</b>	<b>7</b>
<b>INTRODUCTION</b>	<b>9</b>
<b>1. GENERAL CONCEPT OF DAMAGE MODELING IN INTERNAL COMBUSTION ENGINES</b>	<b>11</b>
<b>2. LOCAL DAMAGE RESULTING FROM EXPOSURE TO ABRASIVE PARTICLE</b>	<b>15</b>
2.1. Some features of air filtration in car engines	19
2.2. Design features that may affect abrasive wear	26
2.3. Features of dust particle distribution in branching inlet channels	27
2.4. Radius model for calculating of dust particle distribution in branching channels	29
2.5. Model of particle distribution along branching channels, taking into account the particle deviation from the streamlines	33
2.6. Modeling of particle redistribution in branching inlet channels using the radius model	34
2.7. Simulation of two-phase air flows with dust particles in the engine intake system using a numerical method	40
2.8. Model of two-phase air flow with dust in a channel with a side outlet of 90 degrees	41
2.9. Simulation of two-phase air flow with dust particles at different angles of the flow rotation	53
<b>3. LOCAL DAMAGE WHEN LIQUIDS ENTER THE ENGINE CYLINDER</b>	<b>63</b>
3.1. Model of connecting rod damage during hydraulic lock depending on the amount of liquid entering the cylinder	67
3.2. Influence of connecting rod material and geometry on the nature of damage	76
3.3. Results of modeling of air parameters with liquid in the cylinder	78
3.4. Determination of loads acting on the piston and piston pin during hydrolock	83
3.5. Modeling of the deformation process of the parts of the engine connecting rod-piston group during hydrolock in the cylinder using the finite element method	97
<b>4. LOCAL TEMPERATURE DAMAGE IN ENGINES</b>	<b>113</b>
4.1. Modeling the process of engine damage during an emergency coolant leak	119
4.2. Model of heating of the temperature sensor, combustion chamber wall and piston head during cooling failure	125
4.3. Modeling of unsteady heating of engine elements after a cooling failure	129
4.4. Model of the temperature state of the valve head with changing modes by the valve timing control program	131

4.5. Simulation of the valve thermal damage during failure of the variable valve timing system	142
<b>5. LOCAL DAMAGE TO BEARINGS DUE TO ENGINE LUBRICATION SYSTEM FAILURE</b>	<b>147</b>
5.1. Evaluation of the centrifugal force influence on bearing lubrication	152
5.2. Model of changes in oil supply pressure to bearings after oil system failure	154
5.3. Simulation of bearing damage due to lubrication system failure	159
<b>6. EXPERIMENTAL RESEARCH OF PERFORMANCE FAILURES IN AUTOMOTIVE INTERNAL COMBUSTION ENGINES</b>	<b>163</b>
6.1. Statistic analysis of performance failures in automotive internal combustion engines	163
6.1.1. Warranty operation period	165
6.1.2. Post-warranty operation period	171
6.2. Spare parts nomenclature formation at automobile transport enterprises	180
6.3. Engine coupling wear assessment	189
<b>CONCLUSION</b>	<b>203</b>
<b>REFERENCES</b>	<b>207</b>

## LIST OF SYMBOLS

$u, v, w$  – flow velocity, m/s;

$p$  – static pressure, Pa;

$V$  – volume, m<sup>3</sup>;

$T$  – absolute temperature, K;

$m$  – mass, kg;

$P, F$  – force, N;

$M$  – moment, Nm;

$\rho$  – density, kg/m<sup>3</sup>;

$t$  – temperature on the Celsius scale, °C;

$\tau$  – time, s;

$\varphi$  – crankshaft rotation angle, degrees (rad);

$\omega$  – angular velocity, rad/s;

$n$  – crankshaft rotation speed, rpm;

$l, L$  – characteristic linear size, length, m or mm;

$d, R$  – diameter and radius, mm;

$f, F$  – area, m<sup>2</sup>;

$G$  – gas, particles mass flow, kg/s;

$\xi, \mu, \varepsilon$  – coefficients of hydraulic resistance, flow rate, liquid filling;

$\beta, \gamma, \varphi$  – angle, degrees;

$\sigma$  – stress, MPa;

$\delta$  – thickness, axial deformation, m or mm;

$\psi$  – longitudinal bending, mm;

$\nu$  – coefficient of kinematic viscosity, m<sup>2</sup>/s;

$Q, A$  – amount of heat and work, J;

$U$  – internal energy, J;

$C_p$  – specific heat (heat capacity) at constant pressure, J/(kg·K);

$k$  – heat capacity ratio;

$q$  – specific heat flow, W/m<sup>2</sup>;

$\alpha$ , W/(m<sup>2</sup>·K);

$\lambda$  – thermal conductivity coefficient, W/(m<sup>2</sup>·K);

$C_D$ – aerodynamic drag coefficient;

$Re$  –Reynolds number;

$Nu$ – Nusselt number;

$Pr$  – Prandtl number

$Q$  – air consumption

$P$  – pressure, kPa

$R$  – gas constant of air

$k$  – adiabatic index (for air)

$h$ – wear,mm

$\Delta$  – value of the installation gap in the ring lock, mm

$W$  – wear, mg

$L$  – the value of the diagnostic parameter “leakage” when the piston is on the compression stroke

$\eta_k$  – kinematic viscosity of oil, cm<sup>2</sup>/s;

$q_{OP}$  – the performance of the oil pump

$\eta_h$  – hydraulicpumpefficiency

$K_T$  – temperature coefficient

## **PREFACE**

The monograph examines a number of previously unnoticed and insufficiently studied mechanisms for the development of faults that cause local operational damage in automobile internal combustion engines.

The book consists of six sections (chapters).

The first section provides a general concept for modeling the processes and mechanisms of the occurrence and development of engine faults. The role, capabilities, purpose and features of mathematical modeling of processes that lead to damage and failure of engines are determined. The difference between modeling operational engine damage and modeling during design and research work is shown.

The second section of the book is devoted to local abrasive wear from the redistribution of dust particles in the inlet pipelines under the influence of centrifugation when the air flow turns into side outlets. A “radius” model is presented for calculating the trajectory of a single particle with a deviation from the lines of air flow that moves along the radius. Simulation of the 2-phase air flow with particles was performed using the finite volume method, which generally confirmed the data obtained using the radius model. This phenomenon characterizes the mechanism of abrasive wear, caused exclusively by a local increase in the abrasive action of particles. It is noted that this can lead to catastrophic wear in the engine even with completely normal air filtration and wear resistance of rubbing parts.

The third section of the book discusses in detail the models of the occurrence and development of damage when various liquids enter the engine cylinder. Attention is paid to both thermodynamic models and models of the stress-strain state of the connecting rod stem during loss of stability. A model of local damage to parts of the connecting rod-piston group and a model of deformation of the connecting rod when liquid enters the internal combustion engine cylinder (hydrolock) have been developed in detail. The dependence of the deformation value on the coefficient of filling the combustion chamber with liquid was obtained. Using modeling, the deformation values of the connecting rod stem, piston skirt and piston pin under overload caused by hydraulic lock were established. Thus, the proposed model makes it possible to objectively assess the residual deformation of engine parts and provides a fairly complete and objective picture of the process of deformation and destruction of engine parts during hydraulic lock. This allows us to explain the complex destruction of not only the connecting rod, but also the piston skirt and piston pin.

The fourth section describes the model and results of the simulation of local thermal damage to engines. The developed cooling system failure model made it possible to objectively reproduce the mechanism of the failure with local damage to the combustion chamber of the engine cylinder in the form of melting walls, the appearance of cracks, and loss of valve seats. When simulating local thermal damage to the intake valve during the failure of the valve timing control system, a noticeable increase in the temperature of the

valve head relative to the operating temperature was noted in full valve opening modes. It has been established that a local increase in valve temperature only due to a decrease in the duration of the intake phase and the valve lift height can lead to thermal deformation (creep) of the valve and engine failure.

The fifth section examines local damage to engine bearings and describes a model of oil flow through the crankshaft channels in the field of centrifugal forces, which is adapted for typical crankshaft designs. The model showed the maintenance of oil supply to the connecting rod bearings for a certain time from the moment of failure in the lubrication system, which depends on the design and operating mode of the engine. The simulation results made it possible to explain the difference in lubrication conditions and the degree of damage to the main and connecting rod bearings in emergency cases of oil supply failure. This is key information for a number of practical cases when determining fault causes.

The sixth chapter is devoted to the consideration of the results of engine malfunctions experimental studies on the example of a particular transport company during the warranty and post-warranty vehicle operation periods. It was determined the regularities of malfunctions of components and parts. The issues of the need to store spare engine parts at a car service enterprise are considered, and it was assessed the wear of the joints.

Based on the results of the research, it was noted that the developed models can be used in practice in determining the fault causes of various type engines, and their use in expert studies can increase the accuracy and objectivity of expert conclusions. Thus, the book combines currently available information on mathematical models of the occurrence and development of various engine faults, taking into account the characteristics of studies carried out within the framework of forensic and extrajudicial examinations of the vehicle technical condition.

The book is intended for undergraduate, graduate and postgraduate students as well as researchers majoring in Automobile operation, but may also be useful to engineers, experts, scientists and specialists in other fields related to the process research, design and operation of internal combustion engines.

## **INTRODUCTION**

When creating new automotive internal combustion engines, it is customary to use 3D modeling to determine both the existing loads and the characteristics of air and gas flow in order to optimize the designs and their characteristics. However, practice shows that not all features of the operation of a real structure under real operating conditions can be taken into account using the known models.

This paper discusses the mechanisms of occurrence and development of such faults, which are accompanied by local damage to engine parts and assemblies. Among them, one of the main places is occupied by the process of air purification (filtration) in the intake system of modern engines. A characteristic feature of this process is that even the use of the highest quality filters cannot completely eliminate the entry of abrasive particles into the engine. Meanwhile, this feature can have the most negative and decisive impact on the service life and reliability of a car engine.

In the practice of expert research on the failure causes of a large number of automobile engines, cases were noted in which significant abrasive wear was detected in the engine in the absence of obvious breakage of the tightness of the intake system elements. Such cases often baffled expert researchers who were investigating to determine the cause of the fault. This especially applies to damage that is purely local in nature, when damage is concentrated in a single place, for example, within one cylinder of a multi-cylinder engine. Local damage also includes hydrolock in the cylinder from liquid ingress, discussed in detail in the work, as well as impaired cooling of various elements and various types of bearing lubrication problems.

Indeed, most often such cases are attributed to engine manufacturing defects. Which is understandable – if the malfunction is local in nature, local damage becomes a fairly important sign of a manufacturing defect. For example, a defective part in one of the cylinders causes local damage in that particular cylinder, with minimal expansion of the damage zone to other engine cylinders. Moreover, the engine fails, as a rule, with relatively little operating time (car mileage).

However, practice shows that behind the apparent simplicity of the processes that easily explain such occurrences, there is, in fact, a completely different reason. It means, for an explanation, it is necessary not only to make an effort to analyze all the signs of damage, but also to create mathematical models of processes in order to simulate them. Only then can we find some previously unidentified patterns in order to correctly explain the mechanism of the processes.

This is exactly what happens with the local damage considered in the present study. For example, the concurrence of signs of a malfunction can greatly complicate the correct determination of its cause, which is often the case in practice, when in order to correctly determine the cause it is necessary to look for other signs that confirm any given version under consideration. That is why cases of identifying anomalous types of signs have caused

the need, on the one hand, to explain their occurrence, on the other, to develop algorithms for their study and modeling, and on the third, to determine the possibilities and ways to eliminate or at least reduce their harmful effects of reliability and durability engines.

This work is devoted to solving all the aforementioned problems.

## **1. GENERAL CONCEPT OF DAMAGE MODELING IN INTERNAL COMBUSTION ENGINES**

During the operation of vehicles, a large number of malfunctions arise that are associated with exceeding maximum operating modes, including breakage of operating conditions. The main task of researching engine technical conditions within the framework of automotive technical expertise is to search for and determine the fault cause.

The occurrence of an engine fault in the operation of a modern car often leads to a breakage of a number of functional parameters and usually causes a reaction from the self-diagnosis system by recording an error code and triggering a malfunction lamp (MIL).

At the stage of damage occurrence and its initial development, a self-diagnosis system can be useful for localizing the malfunction for the purpose of subsequent determination of the cause. Indeed, modern self-diagnosis systems of some vehicles make it possible in some cases to record and identify the moment of initial operational damage, from which it is sometimes even possible to obtain the exact time of the initial damage to failure.

Practice shows this can be done both in the initial period after the initial damage and after its development and failure. However, it is most often impossible to use this data to create any quantitative patterns due to the influence of the design features of specific internal combustion engines, operating mode safter damage, the features of recording and storing information in most self-diagnosis systems (including erasing information after removing electric power) and, as a consequence of significant difficulties in collecting the necessary statistics. As a result, the expert researcher often encounters only the final result of the failure, for example, with a large number of fragments of destroyed parts – connecting rods, pistons and valves. And in some cases, it may be an engine that has already been dismantled and disassembled when it is not possible to obtain and use diagnostic data.

An analysis of the procedure for expert studies of various faults [1, 2] also shows that the correct determination of their causes and the construction of any methods is impossible without a detailed description and analysis of all their signs. It is important that it is impossible to solve the direct problem, namely, only by the nature of destruction (fracture) of individual parts, to determine the reason why they turned into fragments. In this case, an attempt to approach the solution of the problem in exactly this way is a typical mistake of experts, which does not allow correctly identifying the cause of the failure. It is not surprising that, given such difficulties in determining the causes of engine failures, a “descriptive” approach in research has become widespread, when, instead of carrying out calculations, a description of the process under study is given. Typically, such a description is taken from available sources, most often from textbooks, and the interpretation of the provisions of the theory can be quite free and allow unverified explanations to confirm the necessary conclusions.

The reason for this simplified approach is related, on the one hand, to the lack of methods and calculation models with which one could confirm any given hypothesis of the cause of failure. At the same time, attempts to apply known methods and models for calculating abnormal conditions that are caused by breakage of operating conditions rarely help. Such models are usually developed from the analysis of the normal engine operating conditions and do not cover areas or cases of significant deviation from them.

On the other hand, it should be taken into account that conducting an expert study to determine causes of failure is usually limited by strict time frames and the capabilities of the given expert. This does not allow the use of complex models, which are usually used in research and design practice and require lengthy special training and significant financial costs for the acquisition of special programs. In addition, the established practice of expert research, including forensic examinations, does not require the expert to use calculation methods and models to substantiate certain hypotheses put forward by him to explain the processes under study. Along with the lack of models and research methods, this creates difficulties in proving the versions of the causes of some faults.

As a result, the task of developing methods and models, although important, must be solved, taking into account the real possibilities of using methods in the practice of expert research. In other words, the developed models should be quite simple, accessible and they should not require significant resources for their implementation when conducting expert studies of the technical condition of engines in operation.

This can be achieved, in particular, by theoretical study of certain faults that are often encountered in practice, in order to develop methods and calculation models for the theoretical justification of various damages received by engine parts. In addition, to verify and/or refine the developed models, it is necessary to use standard programs (software) and modern methods of computer modeling, including 3-dimensional. It concerns both flow of working gases and liquids, and the stress-strain state of parts. For this reason, when developing models, it is advisable to use the simplest versions of the programs, and consider the processes of damage to parts when working under abnormal conditions with a number of simplified assumptions.

The development of models describing damage processes in internal combustion engines should be based on the basic physical laws of mechanics, thermodynamics, gas dynamics, hydraulics, strength of materials and other general engineering sciences. For example, modeling internal combustion engine processes, especially when it comes to thermal processes, cannot be done without the law of conservation of energy (heat balance).

For many practical problems, it is also necessary to estimate heat losses in the walls of the combustion chamber. This is especially important when modeling intra-cylinder processes, for which it is necessary to calculate the heat transfer coefficient from the gas into the wall of the combustion chamber. At the same time, many parts of the internal combustion engine are connected to each other, and contact heat transfer occurs on the mating surface. Extreme conditions occur in the area of contact between the valve and the

seat, because when the contact is broken, overheating and damage to the valve is possible. This determines the importance of mathematical description and modeling of the damage mechanisms associated with violation of contact conditions.

To simulate intra-cylinder processes, there are many standard programs for calculating the operating engine cycle (AVL-Boost, Ricardo WAVE, GT-Power, Lotus Engine Simulation, etc.). However, their main use has traditionally been limited to research and design tasks and rarely extended to issues of operation and, even more so, fault modeling. The equations used in such programs are derived from the law of conservation of energy (1st law of thermodynamics) and the ideal gas equation of state. Moreover, the thermodynamic models that are implemented in these programs usually calculate the one-dimensional flow of gas in the intake and exhaust channels adjacent to the cylinders. This makes it possible to take into account dynamic (wave) phenomena in pipelines and their influence on processes in the cylinder. For operational purposes, this is important because it determines the conditions of heat exchange on the parts, including valve heads.

When studying damage that occurs when operating conditions are broken, issues of the strength of parts become of particular importance. It is known from practice that many initial damages develop over time and end in fatigue failure of the part. In some cases, the emergency impact is instantaneous, and then high loads on parts made of structural materials can cause plastic deformation. If the equivalent stress in any element of a part exceeds the yield strength of the material, it means a loss of strength and the appearance of residual deformations. This fact is important for solving practical operational problems, for example, loss of connecting rod stability.

Some of these processes can be described, for example, within the framework of the classical theory of strength of materials. However, as a rule, theoretical models are much more often used in design problems. At the same time, modeling was not actually used to determine the causes of malfunctions, and the use of models in this area was not justified.

This applies most strongly to 3-D modeling methods. Currently, software systems widely known and widespread in scientific research and design development (Autodesk, SOLIDWORKS, ANSYS, etc.) are usually not involved in any way and are practically not used in operational tasks of studying engine damage. At the same time, some programs (for example, ANSYS), unlike other design programs, allow one to consider the state of internal combustion engine elements far beyond the operating modes. Such a complex can be equally effective both for determining the stress-strain state of parts and in 3-dimensional problems of gas dynamics of internal combustion engines for modeling spatial flows in channels. And if in past years the use of complex programs was limited by the capabilities and speed of computer technology, now the correct formulation of the problem allows one to obtain not only practically important results, but also to check the reliability of the results of simpler models.

In general, to obtain practically significant results, it is necessary to assess the applicability of these models and select the most suitable ones for the problem under

consideration. It is clear that the creation of complete 3-dimensional models of internal combustion engines, modeling of dynamic processes, etc., requires significant software resources, highly qualified users and can be unreasonably complex for operational tasks. However, the use of 3D models is useful for verifying simpler fault models. And this should be done so that the developed methods and models can be subsequently used in expert practice to correctly determine or confirm the causes of engine malfunctions.

## **2. LOCAL DAMAGE RESULTING FROM EXPOSURE TO ABRASIVE PARTICLES**

It is known that abrasive wear is one of the main factors determining the reliability and service life of all types of internal combustion engines in operation [1, 2]. The influence of abrasive wear on the technical condition of engines in operation is confirmed by a well-known fact: for many decades, significant efforts by designers and researchers have been aimed at solving a set of problems associated with abrasive wear of parts and assemblies. These works included the development of measures not only to reduce the supply of abrasive particles to friction pairs, but also to reduce the impact of these particles on rubbing surfaces [3, 4].

Indeed, over many years, all the basic patterns of abrasive wear of friction pairs in relation to internal combustion engines have been studied in sufficient detail, including within the framework of the fundamental scientific discipline that studies friction and wear – tribology [5, 6]. As a result of the research, there were practically no “white spots” left in the processes associated with abrasive wear of internal combustion engine parts. Thus, very specific and comprehensive recommendations have been developed for both identifying (diagnosis) and preventing abrasive wear [7]. This concerns a set of appropriate design measures when designing and creating new engine models in order to organize effective cleaning of air, oil, and working fluids from abrasive particles. In addition to them, technological measures to ensure the wear resistance of parts and assemblies should also be noted [8]. Further, the corresponding activities continue in operation and include the principles and techniques of proper operation of vehicles. This allows you to limit the flow of abrasive into the engine and conduct timely and correct diagnostics of the technical condition determined by abrasive wear. Correct maintenance and repair technologies for identifying and eliminating the consequences of exposure to abrasive particles are also important here [9,10].

On the other hand, it should be noted that the development of internal combustion engines as one of the main types of engines for vehicles for various purposes continues at present under conditions of severe restrictions imposed by economic and environmental requirements. In accordance with this, internal combustion engine designs are evolving quite quickly in the direction of meeting ever new economic rules and environmental standards.

At the same time, it should be noted that previously well-studied patterns from the point of view of counteracting abrasive wear may not fully correspond to the principles laid down when designing new internal combustion engines in a specific modern design. The problem is that such patterns, as a rule, were obtained under other conditions and for other structures. That is, there is a contradiction between the well-studied tribological characteristics of internal combustion engines of old designs and modern economic and environmental requirements, which old designs in general may not satisfy. And such a

contradiction carries the risk of an abnormal and unplanned reduction in the life of new internal combustion engines due to increased abrasive wear.

In addition, in the vast majority of practical cases, abrasive wear is of a general nature, when its effect is approximately the same on all parts of the same type.

Practice shows that specific abrasive wear is also possible, for example, due to the centrifugation of dust in branching channels. Such wear is found in real internal combustion engine designs [1, 2], and it manifests itself especially strongly even with minor violations of engine maintenance regulations and untimely replacement of the air filter.



Fig.2.1. A pipe with flow branching from the air filter to the turbochargers of the right and left rows of cylinders of V-diesel engine

Channels of this type include, for example, the air supply pipe from the air filter of a V-6 supercharged internal combustion engine (Fig. 2.1).

In Fig. 2.2 clearly shows the result of using this pipe in the design of an internal combustion engine – the inlet edges of the compressor blades of the turbocharger, which received air from the far (from the air filter) channel of the pipe, are severely damaged as a result of gas abrasive wear, while the blades of the compressor getting air through the side outlet are practically not have wear.

It is important that in the case under study, a fibrous air filter was used, but its combination with a pipe, which has an obvious and completely harmless, at first glance, design, actually turned out to be of little use for the engine in real operating conditions. As a result, the service life was reduced several times, not only for one of the turbochargers, but also for the entire engine as a whole (cylinder parts that received additional dust amounts also had increased wear).



Fig.2.2. Selective gas-abrasive wear of the inlet edges of the compressor blades of one of two turbochargers over 42000 km of vehicle mileage [9]



Fig.2.3. Intake manifold with variable channel length for a V-6 gasoline engine

An even stronger influence of dust particle inertia on their redistribution along the channels is found in some designs of intake manifolds. Thus, compact designs using additional charging of cylinders by changing the channel length (Fig. 2.3) are characterized by high air velocity in the manifold. In this case, a kind of multiplication of abrasive wear occurs due to the properties of modern fiber air filters described above, when an increasing number of abrasive dust particles can enter the intake system of the internal combustion engine over time. Such particles not only themselves lead to abrasive wear, but can also cause even greater local wear due to inertia by redistributing them to the last (downstream) cylinders.



Fig.2.4. Extremely strong selective (local) abrasive wear of piston No. 1 over 80000 km, while there is almost no wear on other cylinders

As a result, so much dust can accumulate in one cylinder that the life of its parts (and the internal combustion engine as a whole) due to abrasive wear will decrease many times (Fig. 2.4) compared to other cylinders, the life of which, on the contrary, will increase. This can lead to premature internal combustion engine failures due to extremely severe abrasive wear in only one cylinder, even within the manufacturer's warranty period.

In Fig. 2.5 shows the pistons of cylinders Nos. 1, 3 and 5, as well as valves from cylinder No. 1 of a 3,5 liter V6 engine after a vehicle mileage of 24013 km under operating conditions [1] when using the so-called “zero resistance” air filter [2]. The engine was taken out of service due to excessive oil consumption, which exceeded the permissible level of 1 liter per 1000 km.

The data obtained indicate that the working surface, piston rings and piston grooves are most worn out in cylinder No. 1. Slightly less wear in cylinder No. 3 (the upper rings in these cylinders were broken at the lock due to vibrations caused by an excessive increase in clearance in conjunction with a broken piston groove). At the same time, in the other 4 cylinders the wear is much less or even within acceptable limits.

Noteworthy is the wear of parts in cylinders No. 1 and 3 – it is many times greater than in other cylinders. Engine parts of this model wear out in exactly the same way as a standard air filter if the rules for replacing them are violated, with the only difference being that wear occurs over a longer period of time. In other words, in the described cases, wear does not have a general, but rather pronounced local character, acting selectively only on some parts.

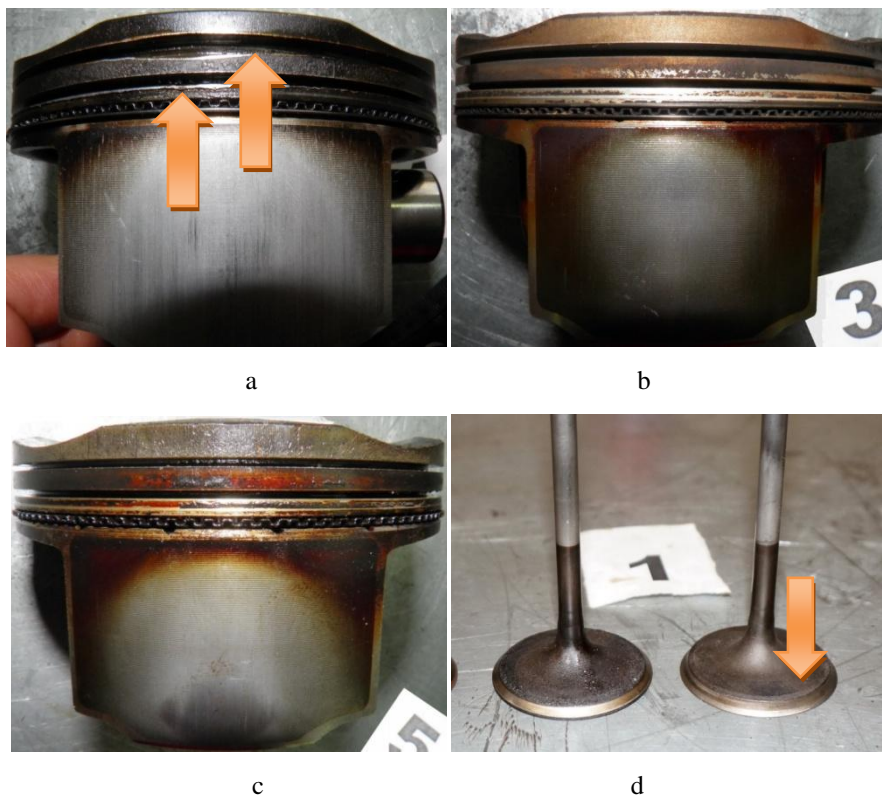


Fig. 2.5. Pistons and valves of a V6 engine with the manifold shown in Fig. 10, after operation with a non-standard air filter: a – piston No. 1 (arrows indicate extremely worn ring grooves), b – piston No. 3, c – piston No. 5, d – valves from cylinder No. 1 (the arrow shows a heavily worn valve located further from the entrance to the manifold)

In fact, experimental data obtained in expert studies show that dust has not only abrasive properties, but also particle inertia. Because of this, particles due to centrifugation can be unevenly distributed over the structural elements of the intake system of the internal combustion engine and concentrated in one of the cylinders, which sharply increases the wear of its parts. As a result, the durability of the engine is sharply, significantly reduced and, thus, depends not only on the wear resistance of all parts and the efficiency of the air filter, but also on the design of the intake system.

## 2.1. Some features of air filtration in car engines

To determine the quantitative characteristics of the phenomenon, it is necessary, first of all, to find the sources of abrasive particles. This requires consideration of the design of modern air filters.

It is known that abrasive wear in an engine is caused by fine abrasive particles larger than 5 microns in size [11], so the main task of the air filter is to remove all such particles from the air. For this purpose, any air filter consists of two parts – a base, which gives the filter rigidity but does not participate in the filtration process, and a filter material with a developed surface.

It is generally accepted that the air filter should almost completely or at least with some maximum possible efficiency, clean the air entering the engine from abrasive particles. Indeed, in engines of previous years of production, paper filters [12] became widespread, the operation of which is based on the mechanism of direct retention of dust particles (Fig. 2.6).

Direct particle retention was based on the so-called “sieve” effect, where all particles that are larger than the pore size or the distance between the fibers in the filter are caught and retained (Fig. 2.7).



Fig.2.6. Traditional paper air filters are based on particle retention using a sieve effect

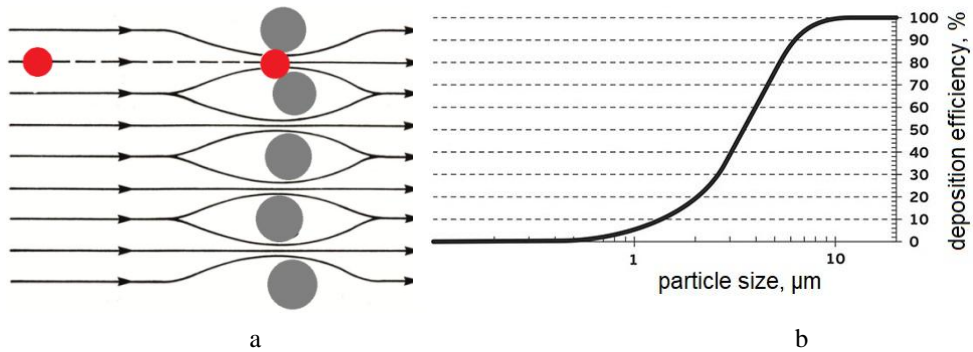


Fig. 2.7. Scheme of direct retention of particles which are larger than a given size by the pores of the material (sieve effect [13]): a – mechanism for retention of particles larger than a given size; b – filter efficiency depending on particle size

It is clear that if, in the initial period, the filter retains all dust particles at a size larger than the specified one, then as contamination increases, the size of the particles retained by the filter will decrease. As a result, the main characteristics of a paper air filter, i.e. cleaning efficiency and screening fineness, increase with mileage, which in general ensures high quality air purification in operation.

However, this useful property of paper filters also entails disadvantages, including a relatively small dirt holding capacity and a rapid increase in hydraulic resistance as they become dirty [10, 14, 15]. It is clear that an increase in resistance leads not only to a decrease in the amount of incoming air, but also to losses in the power and environmental characteristics of the engine.

These shortcomings, coupled with increasing environmental requirements, led to the gradual replacement of traditional paper air filters with filters made of so-called “non-woven” synthetic fiber (Fig. 2.8). It has randomly arranged fibers of different thicknesses, approximately 0.5-5 μm, with a distance between them of about 10-50 μm [8, 11, 16]. Such filters are also called non-fixed pore filters, since the distance between the fibers varies greatly, the fibers themselves do not have any special weave with each other and, thus, have the possibility of mutual movement.

But the main difference between fiber filters and paper filters is in the filtration process. Now, for filtration, a particle does not have to get stuck in the fibers, if it just touches the filter material, this is already enough for effective sedimentation. As a result, effective filtration occurs at a distance between fibers that significantly exceeds the particle size [11, 17].

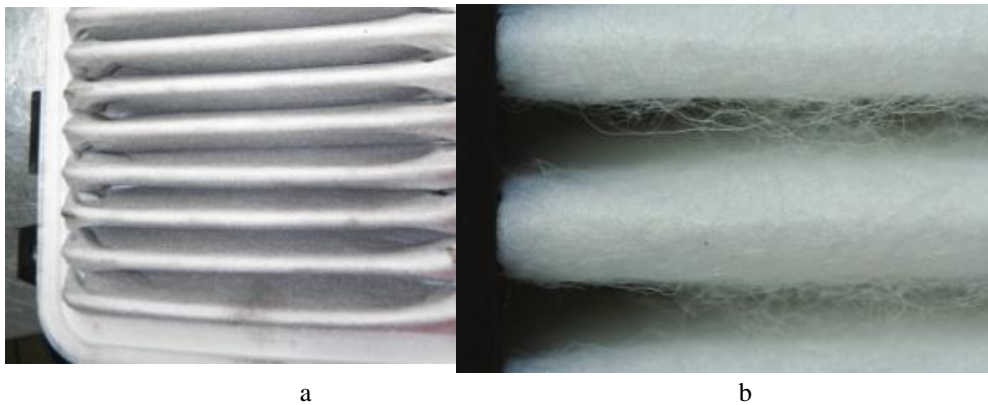


Fig.2.8. Air filter made of non-woven fibrous material (a) and the magnified texture of the fibers (b)

Such properties of fiber filters are associated with several processes, including adhesion, diffusion, inertia (Fig. 2.9) and other effects [13, 16, 17].

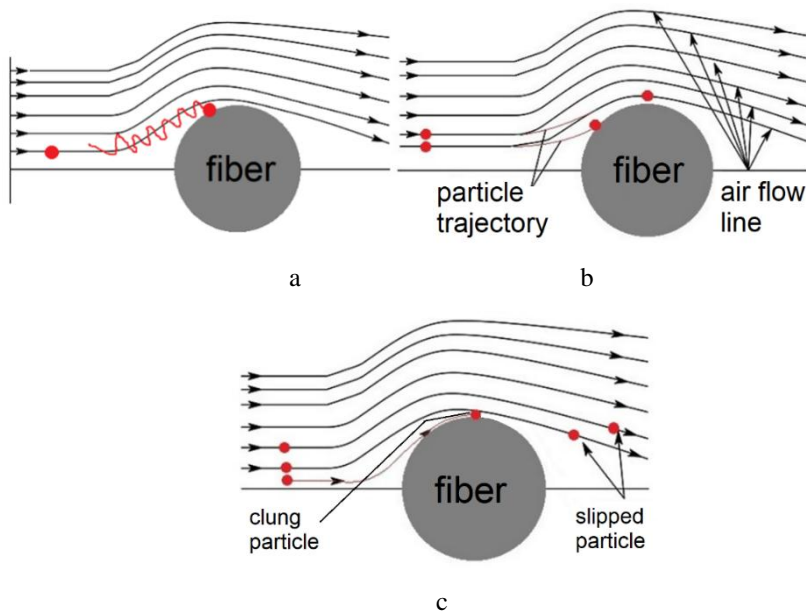


Fig.2.9. The main effects on which the operation of modern fiber filters is based [10]: a – diffusion; b – inertia; c – clingage

An analysis of all the effects used in filtration (Fig. 2.10) shows that the efficiency of the filter depends not only on the size of the filtered particles, but also on the parameters of the filter itself, including the diameter of the fibers in the filter and the packing density of the fibers.

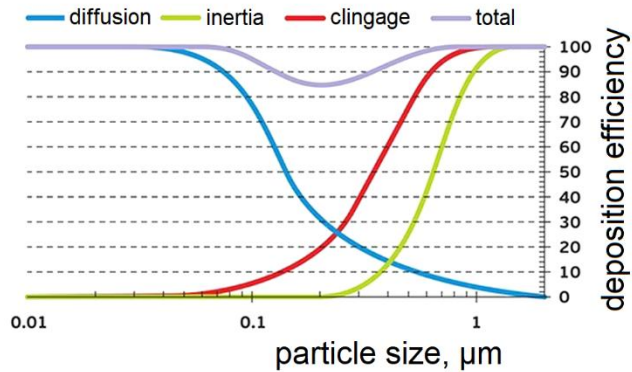


Fig.2.10. The influence of particle size on filter efficiency under the combined action of several effects

Obviously, the thinner the fibers and the more densely they are packed, the greater the area of their contact with the particles. And the better the fibers cling to the particles, the more effective their deposition. But as particles settle, the distance between the fibers decreases, the surface of the fibers becomes cluttered, and their area increases. This may be due to the deterioration of the filtration efficiency over time of operation [12]. Since dust particles do not clog the pores, but stick to the fibers [11, 17], noticeable clogging of the fiber filter does not occur over time, and the flow sections between the fibers remain to one degree or another free (Fig. 2.11). Accordingly, there is no noticeable increase in the hydraulic resistance of the filter during operation as it gets dirty, and its impact on engine operation remains minimal.

Despite these advantages of fiber air filters, over time, their disadvantages also appear. When the fibers become heavily contaminated with particles deposited on them (Fig. 2.11), they lose the ability to retain abrasive particles using the effects described above. In addition, under certain conditions (for example, mechanical stress), fibers can release accumulated particles into the filtered air [16]. All these features of fiber filters cause a gradual increase in the passage of more and more abrasive particles into the engine.

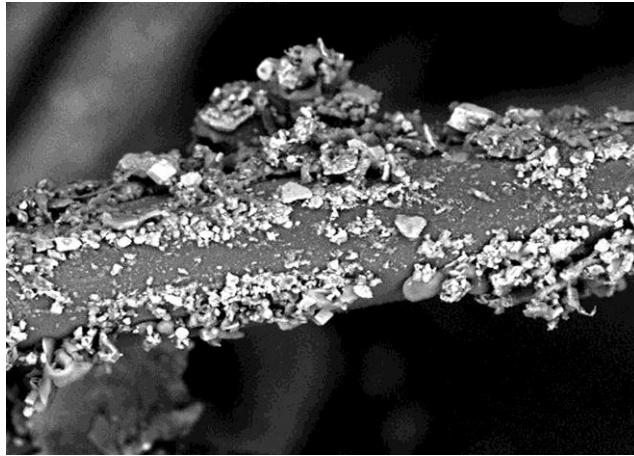


Fig.2.11. The particles which cling to the surface of the fibers when the filter is dirty [17]

Even if the pressure increases smoothly and not by too great an amount, the release of accumulated particles is more likely if the pore sizes of the filter material increase during deformation. Existing filter elements prone to similar phenomena, i.e. to release particles, are usually made of a filter material with many fibers, loosely bonded together, and which can move when pressure increases.

This process is probabilistic in nature, and in general, the release of filter-accumulated particles in non-woven fibrous materials is more likely if the pores of the filter material can increase with increasing pressure drop. In addition, filter materials of all types also capture particles smaller than the pore size. Under certain conditions, such accumulated fine particles will be less well retained if the pores of the filter material can become larger.

This is the well-known problem of filter materials with unfixed pores [7, 11, 13]. These filter media have many tortuous channels through which air can pass in different ways. Naturally, narrower channels become blocked (filled with particles) earlier, causing an increasingly larger portion of the flow to flow through increasingly wider channels. Since such filter materials are not structurally one unit, increased pressure drops within wider passages can disrupt the structure, and therefore widen those passages. Obviously, this circumstance negatively affects the characteristics of the filter.

The filtering characteristics of materials with non-fixed pores depend not only on the possibility of retaining particles, but also on the possibility of their adsorption. As long as the forces acting on the retained particles from the filtered medium are less than the forces retaining these particles in the filter material, the particles remain fixed in it. However, during the operation of the filter, a certain number of particles accumulate in the filter

material. If there is a sudden change in flow or pressure, the impact of the filtered medium may exceed the holding forces, and some particles will be carried away by the flow of the filtered medium. Due to the discharge of accumulated particles into the stream leaving the filter with some frequency, a false impression may be created that this filter has a high resource and service life.

Most filter materials with a non-fixed porous structure are characterized by migration of the filter material into the filtered air. This means that particles/fibers of the filter material are separated from it and carried away by the flow of the filtered medium, contaminating the filtered air. The migration of filter material into the filtered medium is often mistakenly associated with the removal from the filter material of “original” contaminants, for example, dust and fibers that entered the filter during its production.

In addition, a dirty filter with fibers on which a large number of particles have already settled loses the ability to trap and retain small particles due to the effects of adhesion, diffusion and electrostatic forces, since the particles deposited on the fibers and covering them block the action of the fibers on the particles, located in the flow of the filtered medium (Fig. 2.12).

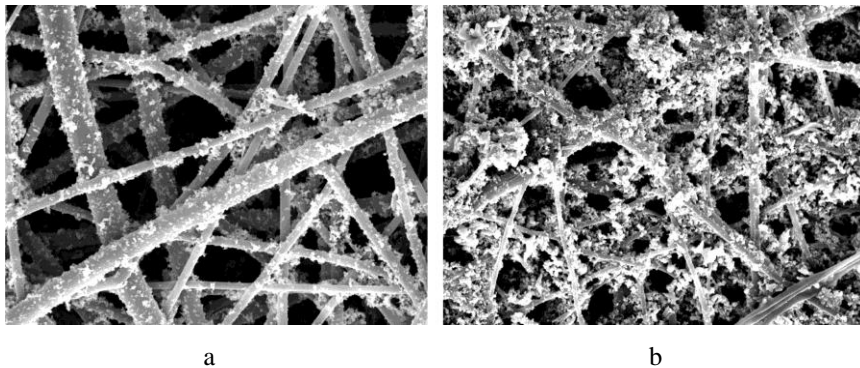


Fig. 2.12. Filter fibers after a short operating time (a) and before replacement (b). If the fibers are dirty, they lose their ability to trap small particles, and such particles can pass unhindered into the engine [2]

The gradual blocking of narrow channels by particles described above results in the direction of small particles into larger channels that do not effectively filter small particles.

Thus, if old paper filters showed an increase in cleaning efficiency over time with increasing resistance, then modern fiber filters should highlight a gradual deterioration in overall cleaning efficiency as the main feature. The change in characteristics of filters of different types during operation is illustrated in Fig. 2.13. If the main problem of a paper filter was the rapid increase in hydraulic resistance near the operating limit, then a non-

woven fiber filter experiences a drop in the efficiency of particle sedimentation (filtration), while the hydraulic resistance of the filter may not yet reach critical values.

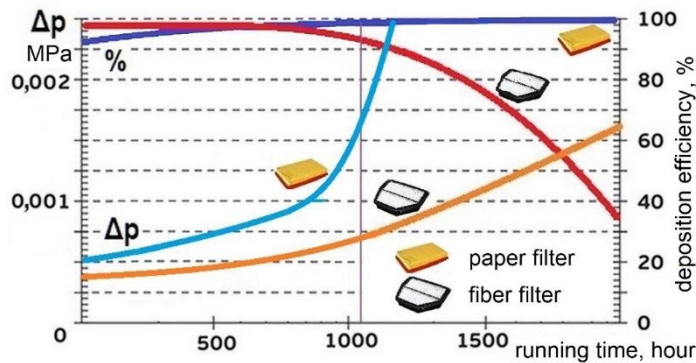


Fig.2.13. Approximate pattern of the change in pressure drop and filtration efficiency of a fiber filter in comparison with a paper filter during engine operation

This feature of the non-woven filter has a beneficial effect on the operation of the fuel supply system and the environmental characteristics of the engine. However, a decrease in filtration efficiency can become a real threat to reliability and durability. This is due to the absence of clearly visible external signs of pollution, when continued operation of the engine with a dirty air filter can lead to abrasive wear and a noticeable reduction in service life.

However, when searching for patterns, it is important to analyze not so much the susceptibility of engine parts to abrasive wear (it has generally been studied in detail), but rather the ability of various design elements to influence abrasive wear of parts and reduce engine life. It is necessary to take into account that many engine designs, as well as their design principles [18-22], have remained unchanged for many decades, while the spread of fiber filters occurred relatively recently, 10-15 years ago. This means that simply switching from paper filters to fiber filters, with the engine design unchanged can cause new malfunctions that have not previously been encountered or described.

## 2.2. Design features that may affect abrasive wear

For a long time, in the practice of designing and operating internal combustion engines, it was assumed that the air entering the engine, after proper cleaning with an air filter, was free of dust particles. Then the dust does not have any effect on the processes occurring during the entire service life of the engine. Conversely, in the case of problems with cleaning the air from dust, the engine could be subject to accelerated abrasive wear.

Analysis of sources shows this model is simplified, i.e. does not take into account the influence of dynamic processes in the intake system on the wear of engine parts, but has become widespread. This is confirmed by the fact that significant efforts have traditionally been focused on studying the abrasive wear of parts and ways to reduce it as the main way to improve the reliability and durability of engines [23]. On the one hand, this route involves imparting high wear resistance to friction pairs [22], and on the other hand, it requires increasing the efficiency of air purification [24]. Moreover, the fact that the flow of air with dust particles is 2-phase (such a flow is studied in detail in applications for industrial centrifugal cleaning [25, 26]). This is not taken into account at all in many studies of internal combustion engines, although these features may have an impact on abrasive wear and durability of engines.

Indeed, the main sources on motor theory, design and failure [19, 21, 27] usually do not mention any problem associated with 2-phase flows. The exception is centrifugal air purification systems and cyclone filters, research into which has been the subject of quite a large number of works [4, 24]. The traditional approach to this problem also assumes that dust can typically affect a car engine, causing abrasive wear when there is some kind of damage to the air filter or intake tract connections. And since this is operational damage, it is, as a rule, of little interest to researchers and designers, who for decades have been creating the designs of engines and their systems, incorporating into the calculation models completely clean air [19, 21, 23].

At the same time, even a simple analysis of the characteristics of the air filters used [13, 16, 19, 28] shows that the air passing through the air filter is very far from a state that could be called “clean”. The paper air filters retain only part of the particles smaller than 20-30  $\mu\text{m}$ , and the smaller the particle size, the more such particles pass into the engine. Modern air filters [13, 14] retain more than 99% of all particles, including the smallest ones. However, as operational pollution occurs, they can gradually lose their properties [1, 7]. This can lead to deterioration in the quality of cleaning and an increasing number of particles entering the engine, including a certain number of previously detained particles [2, 10].

The situation is complicated by the emergence and proliferation of variable-length intake system designs that use dynamic phenomena to recharge the cylinders [2, 23]. In these systems, the intake manifold is no longer a means of smoothing out air pulsations; on the contrary, it can be included in the general oscillatory system, and the air velocities in it can be significant. Under such conditions, uneven redistribution of dust along the intake system channels and cylinders should be expected.

### **2.3. Features of dust particle distribution in branching inlet channels**

Thus, from the principles of operation of some types of modern fiber air filters [11, 16, 17, 29] a peculiarity follows: starting from a certain point in time, contamination of the filter leads to the fact that an increasing number of abrasive particles can enter the intake system, because they will not be delayed by the filter. However, internal combustion engine

intake systems are usually designed with “clean” air, completely free of particles. Such a contradiction can lead in real operations to the redistribution of abrasive particles between cylinders, including the concentration of particles in individual cylinders, and cause a noticeable decrease in service life due to accelerated wear of parts.

It is known that abrasive particles in the size range of 5-30  $\mu\text{m}$  cause abrasive wear of friction pairs, and the size of 10-20  $\mu\text{m}$  is the most destructive for engine parts [8, 11]. However, the question remains unexplored as to what processes in the intake system can be affected by particles from the specified range if their quantity in operation does not decrease, as happened previously with paper filters, but increases. Or, in other words, it is necessary to determine how engine life depends on the properties of the air in the intake system, if the air is not perfectly clean and contains abrasive particles.

It is obvious that any particle with mass, when changing the direction of air flow, can lag behind the air flow lines as a result of the action of inertial forces. In this case, we should expect a redistribution of particles over the cross section of the channel when the flow turns; the particles, by inertia, will be displaced towards a larger radius, i.e. centrifugation of particles will occur [30].

It is easy to assume that this effect will be most pronounced if the channel has side branches, when one should expect a redistribution of particles in favor of rectilinear motion, since the deviation of particles from rectilinear motion is prevented by their inertia.

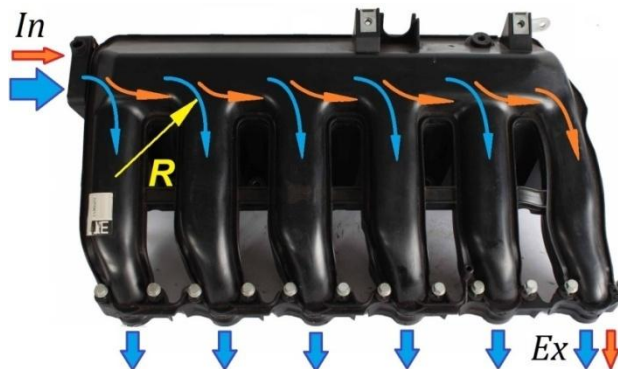


Fig. 2.14. The intake manifold of an internal combustion engine is a typical system in which, with a uniform rotation of air into the side outlets along a radius  $R$ , it is possible to centrifuge dust particles and redistribute them due to centrifugal forces into cylinders increasingly distant from the inlet section  $In$  [2]

Indeed, such design elements, in which centrifugation of abrasive particles is possible, are quite widely used in the intake systems of modern internal combustion

engines. There are various distribution pipes for supplying air to the rows of cylinders, as well as manifolds with pipelines supplying air directly to the cylinders (Fig. 2.14).

It can be assumed that the greatest effect from centrifugation of particles should be expected with sharp turns of the flow with small radius of curvature. With appropriate assumptions, this can be calculated.

## 2.4. Radius model for calculating of dust particle distribution in branching channels

In order to determine possible malfunctions from the uneven distribution of dust particles due to their centrifugation, the movement of a single particle along a curved path (Fig. 2.15) near the side outlet of the channel is considered. This branching of channels in the form of a tee is found in the design of air ducts for various types of engines.

As follows from [32], when the air flow rates in the direct and side pipelines are the same, the flow lines near the outlet are limited by a radius close in magnitude to the width (diameter) of the side channel centered at the corner point (Fig. 2.15).

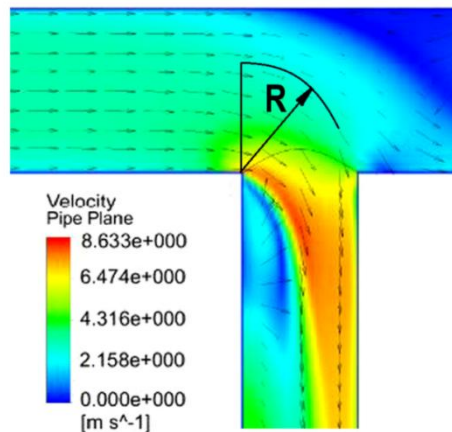


Fig. 2.15. Visualization of the flow during flow branching with the condition of approximately equal air flow rates in the direct and side channels [32]: the flow turning area is limited by a radius close to the diameter of the side channel

In this case, it is possible to draw up a calculation diagram of the problem (Fig. 2.16) in the form of an air flow line with radius  $R$ , and the trajectory of the particle due to centrifugal forces will deviate from the flow line and gradually move to a larger radius. Deviation of the particle's trajectory from the air flow line at the edge of the side channel will cause the particle to “overshoot” past the side channel. It may cause dust particle redistribution when, even at the same air flow rate, a smaller amount of dust will enter the side channel.

### **3. LOCAL DAMAGE WHEN LIQUIDS ENTER THE ENGINE CYLINDER**

From the practice of studying the causes of internal combustion engine failures, it is known that one of the very common causes of severe damage in operation, causing inoperability (failure) of the engine, is the ingress of liquid into the cylinder. This phenomenon has received a common conventional name – hydraulic lock [35, 40, 41].

Despite the completely different causes why different liquids can get into the cylinder, they produce a similar damage process. For example, it is known that hydrolock occurs when the combustion chamber is filled with liquid. Then the piston, most likely, will not be able to reach the upper position (top dead center). Moreover, it will collide with the liquid, which will cause it to stop abruptly, i.e. to hydraulic lock, accompanied by deformation of the connecting rod and damage to other parts [42, 43].

Current experience [35, 44] confirms that when liquid enters the cylinder, the connecting rod stem gets significant axial compressive loads, and can lose stability and deform. An analysis of cases known from the practice of studying the causes of internal combustion engine failures [46,47] shows that the nature of the deformation of the stem can be different in shape for different connecting rods in accordance with differences in the stem profile and flexibility in different directions.

The main symptom of hydrolock is a decrease in the distance between the connecting rod heads due to plastic compression deformation and loss of stability of the stem. This sign completely determines hydrolock, since it is impossible to compress the connecting rod along the axis by any other means in operation. The example (Fig. 3.1) clearly shows that loss of stability of the connecting rod is accompanied not only by bending of the rod, but also by its axial compressing; the interaxial distance between the axes of the crank and piston heads of the connecting rod decreases.

However, making accurate measurements of the deformed connecting rod itself is not easy, and in most practical cases it is completely impossible. The reason is, when the deformation is relatively small, the damage becomes hidden. I.e. the engine can remain operational after hydrolock, but over time, fatigue failure of the connecting rod stem is almost inevitable (most often in its middle section, where the alternating stresses of abnormal bending of the deformed stem are maximal). After that, the measuring loses any sense.

It is clear that in the case of conrod stem fatigue failure (and this is what usually ends the operation of an engine with a deformed conrod), we can only talk about fragments of the connecting rod (Fig. 3.2).



Fig.3.1. The typical shape of the connecting rod stem in the hydrolock in the cylinder after loss of stability



Fig. 3.2. Fatigue failure of the connecting rod after hydrolock does not allow any data to be obtained using direct measurements of the rod

At the same time, it is not necessary to measure the fragments, like the conrod itself, to determine the amount of axial deformation (compression) of the stem. The indirect method is quite suitable for measurements [45]: it is enough to measure the height of the carbon deposits in the upper part of the cylinder and compare it with those cylinders where no hydrolock was detected (Fig. 3.3). In this case, the difference will correspond exactly to the conrod axial deformation.

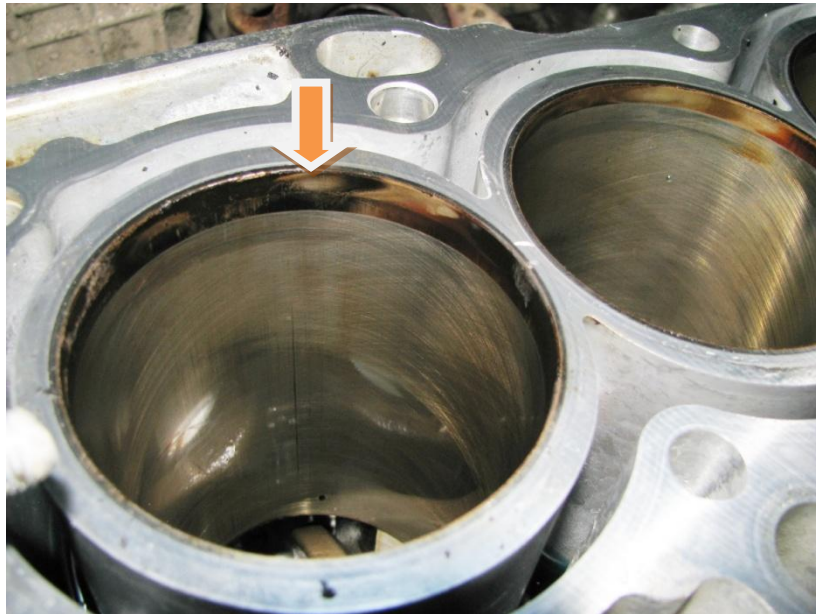


Fig.3.3. The expansion of the carbon deposits in the upper part of the cylinder (on the left) when working with a deformed conrod during a hydraulic lock makes it possible to unambiguously measure its deformation

The measuring of the deformed stem and/or height of carbon deposits on the top of the cylinder can help determine the amount of liquid that has entered into the cylinder.

There are also many other signs of hydrolock that confirm this type of damage. Among them are traces of the piston diagonal operation in the cylinder (Fig. 3.4), similar traces on the conrod bearings, wear on the retaining rings, the ends of the piston pins, the grooves of the retaining rings in the holes of the piston bosses, etc.

In some cases, when a large amount of liquid enters the cylinder at once, the conrod deformation can be significant. Then the piston may be damaged from the bottom side due to its contact with the crankshaft counterweights near the bottom dead center (Fig. 3.5.).

If the engine operation with a damaged connecting rod naturally and quickly ends in its fatigue failure, then an even greater deformation of the conrod stem leads to jamming of the crankshaft right at the moment of hydrolock. In modern automobile engines, the standard gap between the piston bosses and the crankshaft counterweights at the piston bottom dead center is about 3-4 mm. The impact of the piston on the counterweights leaves corresponding signs on the piston (Fig. 3.4), which actually indicate the limiting deformation of the conrod, more which the crankshaft jams.



Fig.3.4. Typical traces of piston operation with distortion in the cylinder after hydrolock

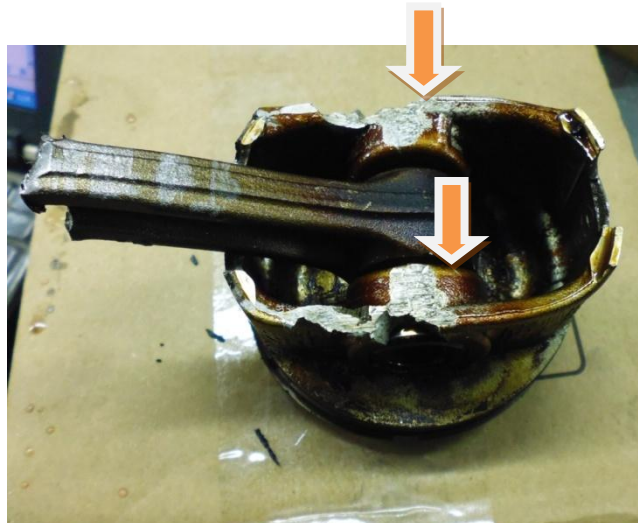


Fig.3.5. Damage to the piston bosses due to their abnormal contact with the crankshaft counterweights after shortening the connecting rod when hydrolock

The damage is most often local in nature, in which the damage is localized in only one cylinder. Only in rare cases does the damage spread to another cylinder, and cases of damage to more than 2 cylinders in a multi-cylinder engine are extremely rare.

At the same time, despite quite numerous references and detailed descriptions of hydrolock in information sources [44, 48, 49, 50], they do not provide any quantitative evaluations or detailed characteristics of this phenomenon. The description of a hydrolock is often limited to only a brief mention of some of its features, and even then, in most cases, incomplete. This is sometimes not enough to practically determine all signs of damage and identify the cause of a specific engine failure, including when conducting an automotive technical expertise exam.

In addition, in known sources there is no data on the influence of the amount of liquid on the magnitude and nature of parts deformation, primarily of the connecting rod. At the same time, known studies of connecting rod deformation [51-53, 54-56] are actually limited only to the deformation itself and do not address in detail the mechanism that causes it [57-61]. As a result, when investigating the failure caused by hydrolock, if you examine the final condition of the parts, it is impossible to determine a single quantitative parameter. Then, if the amount of liquid entering the cylinder is unknown, it is impossible to relate this amount to the existing signs of a specific cause of the hydrolock. And this does not allow us to identify the necessary cause-and-effect relationships with a particular manufacturing defect or operational damage.

To solve these problems, it is necessary to start by determining the nature and magnitude of conrod deformation depending on the amount of liquid entering the cylinder.

### **3.1. Model of connecting rod damage during hydraulic lock depending on the amount of liquid entering the cylinder**

The task of determining the conrod deformation when liquid enters the cylinder can be divided into several stages. At the first stage, it is necessary to consider all the geometric and kinematic parameters associated with the piston movement in the cylinder in the presence of liquid (Fig. 3.6). This makes it possible to compile design equations for the parameters of the air in the cylinder, after which the desired deformation of the connecting rod can be obtained.

It should be noted that similar problems of determining the air parameters in a cylinder have long been solved, and based on their solution, a number of standard programs have been developed for calculating the internal combustion engine cycle [62]. However, it is not possible to use them for the considered process of air compression with a given amount of liquid, since they do not provide for taking into account the influence of the liquid on the compression process. As a result, solving the problem of compressing air and liquid in a cylinder requires the development of an appropriate calculation model.

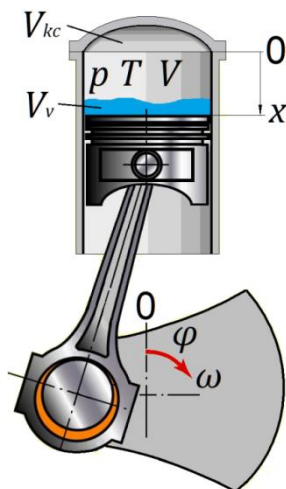


Fig.3.6. When the piston moves upward on the compression stroke, the occupation by incompressible liquid of part of the air volume in the cylinder is a completely expected reason for a more rapid increase in pressure in the cylinder

To solve the task, you must first make simplifying assumptions that will allow you to create the appropriate equations, but, at the same time, will not have a noticeable negative impact on the result. Accordingly, the following simplified assumptions were made:

- 1) the liquid entering the cylinder is incompressible,
- 2) the physical properties of the liquid due to the rapidity of the process do not depend on the temperature and air pressure, the temperature and properties of the liquid are assumed to be unchanged and identical throughout its entire volume,
- 3) in the process under study, the liquid is not subject to evaporation, condensation, chemical reactions and other types of transformation,
- 4) ignition and combustion of fuel are excluded (for example, in an internal combustion engine with spark ignition, any liquid from the above bridges the spark gap of the spark plug and prevents spark discharge. In a diesel engine, the situation is more complicated, but the liquids in question can either also prevent the ignition of the fuel or make its combustion unstable),
- 5) leaks of air and liquid from the cylinder through gaps in the piston rings and valves are not taken into account,
- 6) the instantaneous parameters of the air in the cylinder are the same in volume, their change along the crankshaft rotation angle occurs quasi-stationary,

7) the crankshaft rotation speed is constant and does not depend on the entry of liquid into the cylinder (this is equivalent to the assumption that the crankshaft is heavy and/or its inertia during rotation is very high).

Let us now consider the process of compression of air with liquid in the cylinder from the moment the intake valves are closed, for which we first clarify the geometric parameters. The current volume of air in the cylinder is usually calculated using the formula [21, 63]:

$$V = x \frac{\pi}{4} D^2 + V_{kc}, \quad (3.1)$$

where:  $x$  is the current coordinate of the piston bottom, measured from the top dead center,  $D$  is the cylinder diameter,  $V_{kc}$  is the volume of the combustion chamber.

However, if there is liquid in the cylinder, the formula takes on a different form:

$$V = x \frac{\pi}{4} D^2 + V_{kc}(1 - \varepsilon_v), \quad (3.2)$$

where:  $\varepsilon_v = V_v / V_{kc}$  is the relative volume of liquid (relative to the volume of the chamber), or the coefficient of filling of the combustion chamber with liquid (liquid filling coefficient).

Let's take into account the geometric compression ratio

$$\varepsilon = \frac{V_h}{V_{kc}} + 1, \quad (3.3)$$

where  $V_h = S\pi D^2/4$  is the working volume of the cylinder.

Then, from expression (3.2) we obtain the value of the current volume of air in the cylinder in the form:

$$V = V_h \left( \frac{x}{S} + \frac{1 - \varepsilon_v}{\varepsilon - 1} \right) = V_h A_\varphi, \quad (3.4)$$

where the coefficient  $A_\varphi = \left( \frac{x}{S} + \frac{1 - \varepsilon_v}{\varepsilon - 1} \right)$ .

From expressions (3.3) and (3.4) it is clear that an increase in the amount of liquid leads to a decrease in the volume of air in the cylinder due to its replacement with liquid.

Let us substitute into formula (3.4) the expression for the relative coordinates of the piston bottom. It follows from the kinematics of the crank mechanism of the internal combustion engine [21, 64, 65] depending on the crankshaft rotation angle  $\varphi$ , which is measured from the top dead center:

$$\frac{x}{S} = 0.5 \left[ (1 - \cos\varphi) + \frac{\lambda_c}{4} (1 - \cos 2\varphi) \right], \quad (3.5)$$

where  $\lambda_c = R_{kp}/L_c$  is the relative elongation of the connecting rod,  $R_{kp}$  is the radius of the crank.

Also for the coefficient  $A_\varphi$ , it can be obtained an expression taking into account the replacement of part of the air volume by liquid in the form:

$$A_\varphi = 0.5 \left[ (1 - \cos\varphi) + \frac{\lambda_c}{4} (1 - \cos 2\varphi) \right] - \frac{(1 - \varepsilon_v)}{(\varepsilon - 1)}. \quad (3.6)$$

Let us now consider the air in the cylinder. According to the 1st law of thermodynamics in relation to the compression process in a cylinder under consideration [63, 66]

$$C_p m dT_V = -pdV - \alpha_w F_w (T - T_w), \quad (3.7)$$

The change in the internal energy of air  $dU$  over the process time  $d\tau$  as a result of production of the work  $dA$  on the air and the removal of heat  $Q_w$  from it can be written using the equation

$$dU = dA - Q_w d\tau, \quad (3.8)$$

where is the thermodynamic work

$$dA = -pdV, \quad (3.9)$$

and the change in internal energy is:

$$dU = C_p m dT_V. \quad (3.10)$$

In this case, the amount of heat that is removed from the air into the walls  $Q_w = \alpha_w F_w (T - T_w)$ , the area of the cylinder walls  $F_w = \pi D(0.5D + x)$ , and the mass of air in the cylinder  $m$  does not change during compression, since there are no leaks from the cylinder.

The expression for  $dV$  included in equation (3.7) can be obtained from (3.4) and (3.6):

$$dV = V_h dA_\varphi = V_h B_\varphi d\varphi, \quad (3.11)$$

where coefficient  $B_\varphi$ :

$$B_\varphi = 0.5(\sin\varphi + \lambda_c \sin 2\varphi). \quad (3.12)$$

Equation (3.7) using the expression (3.5) and taking into account the fact that  $\varphi = \omega \tau$ , where  $\omega = \pi n/30$  is the angular velocity,  $n$  is the rotation speed, rpm, can be converted to the form:

$$\frac{dT}{d\varphi} = -T \frac{R B_\varphi}{C_p A_\varphi} - \frac{30 \alpha_w F_w}{\pi n m C_p} (T - T_w). \quad (3.13)$$

We now use the equation of the state of the gas, connecting pressure  $p$ , temperature  $T$  and volume  $V$  of air in the cylinder

$$pV = mRT. \quad (3.14)$$

After differentiating them, we have the equation

$$p dV + V dp = m R dT. \quad (3.15)$$

Next, substituting the expression (3.13) for  $dT/d\varphi$  into equation (3.15), we obtain:

$$\frac{dp}{d\varphi} = -p \frac{B_\varphi}{A_\varphi} \left( 1 + \frac{R}{C_p} \right) - \frac{30 \alpha_w F_w R}{\pi n m C_p A_\varphi} (T - T_w). \quad (3.16)$$

Let us simplify the system of equations (3.15) and (3.16), bringing them to the form:

$$\begin{cases} \frac{dT}{d\varphi} = -T \gamma \psi, \\ \frac{dp}{d\varphi} = -p \gamma \left( \psi + \frac{C_p}{R} \right), \end{cases} \quad (3.17)$$

where the coefficients are:

$$\psi = 1 + \frac{30 \alpha_w F_w R}{\pi n p V_h B_\varphi} (T - T_w), \quad (3.18)$$

$$\gamma = \frac{R B_\varphi}{C_p A_\varphi}, \quad (3.19)$$

and the coefficients  $A_\varphi$  and  $B_\varphi$  are found using formulas (3.6) and (3.12), respectively.

To determine the heat transfer coefficient  $\alpha_w$  from air into the walls, you can use the Voshni formula [63,67, 68]

$$\alpha_r = 128 (10 p)^{0.8} \omega^{0.8} / (T^{0.53} D^{0.2}), \quad (3.20)$$

where  $p$ ,  $T$  are the pressure and temperature of the gas in the cylinder (MPa and K),  $D$  is the diameter of the cylinder, m,  $\omega$  is the speed coefficient proportional to the average piston speed  $C_m = S n / 30$ , assuming at the compression stroke  $\omega_m = 2.28 C_m$ .

The speed coefficient is calculated using the formula

$$\omega = c_1 C_m + c_2 (p - p_K), \quad (3.21)$$

where the values of the coefficients  $c_1$  and  $c_2$  are recommended depending on the phase of the cycle [69],  $p_K$  is the pressure in the inlet pipeline.

The solution of the system represents the numerical values of pressure and temperature as a function of the crankshaft rotation angle of the form

$$p, T(\varphi) = \int_{\varphi=0}^{\varphi=4\pi} f(p, T, \varphi, \dots) d\varphi \quad (3.22)$$

In the 1st approximation, the solution can be obtained by numerically integrating the system of equations (3.22) using the Euler or Runge-Kutta method. To do this, it is necessary to set the integration step over the crankshaft rotation angle  $\Delta\varphi$ , the initial values of temperature and air pressure in the cylinder, which correspond to the moment of closing the intake valves, and calculate the derivatives  $dp/d\varphi$  and  $dT/d\varphi$ . After this, you can determine the pressure and temperature at each subsequent time step by iterations using the formula

$$T_w = T_w + (dT_w/d\tau)\Delta\tau \text{ or } T_{wi} = T_{wi-1} + [(dT_w/d\tau)_i + (dT_w/d\tau)_{i-1}]\Delta\tau/2 \quad (3.23)$$

simultaneously with the calculation of the new current crankshaft rotation angle.

However, the problem under consideration has a peculiarity. The initial conditions for solving the system of equations are the pressure and temperature of the air in the cylinder at the moment of closing the exhaust valves on the compression stroke. These values of pressure and temperature cannot be chosen arbitrarily (including, they cannot be equated to environmental parameters), but must be accurately calculated.

In order to find the initial values of pressure and temperature at the moment of closing the intake valves, it is necessary to calculate the operating cycle of the internal combustion engine using standard programs. To do this, in addition to setting the engine geometry and its operating mode (rotation speed), it is necessary to set the temperature of the cylinder walls  $T_w$ , since it is included in the system of equations (3.17).

Before calculating the initial conditions, it is necessary to determine the influence of the liquid on the intake process. If we consider in detail the entire process of liquid entering the cylinder during the intake stroke, the task will be significantly more complicated. But since we are talking about an approximate model, we can make the simplifying assumption that the volume of the liquid is small compared to the volume of the cylinder. In this case,

the error in calculating the volume of air entering the cylinder will be no more than the ratio of the volume of the combustion chamber to the volume of the cylinder, i.e. no more than 10%.

Consequently, the liquid entering the cylinder during the intake stroke along with the air will not affect the temperature and pressure of the air in the cylinder during this period. As a result, we can accept the condition that during the intake there was no liquid in the cylinder, and it appeared right at the moment the intake ended, simply replacing part of the air in the cylinder.

To calculate the initial values required for hydrolock modeling, the Lotus Engine Simulation program was used [62, 70, 71]. This made it possible to calculate the instantaneous parameters of the thermodynamic cycle of the internal combustion engine (volume-average pressure and temperature in the cylinder) based on the crankshaft rotation angle, in order to then determine the initial conditions for solving the system of equations (3.17) for the value of the crankshaft rotation angle, which corresponds to the closing of the exhaust valves.

When calculating, the data of a typical automobile internal combustion engine were specified [35, 41, 47]: internal combustion engine type is gasoline with spark ignition, engine size is 83x84 mm, compression ratio is 9,0, operating mode is 3000 rpm, closing the intake valves is  $40^0$  after the bottom dead center, wall temperature is 390K and other parameters. Since the purpose of the calculation was not the main integral parameters of the engine (power, torque, specific fuel consumption), but the temperature and pressure in the cylinder, a simplified 1-cylinder model was used (Fig. 3.7).

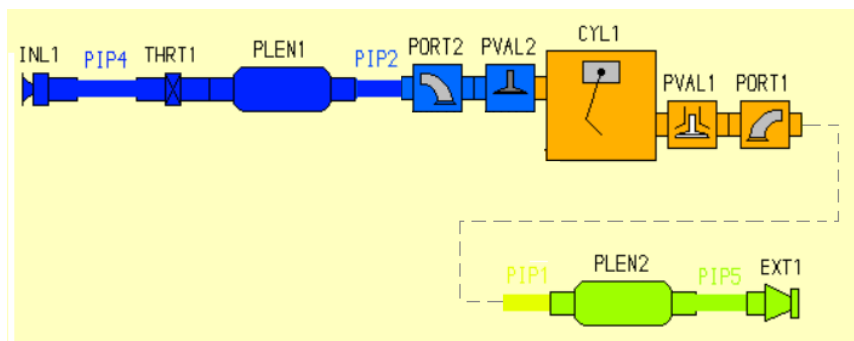


Fig.3.7. 1-cylinder geometric engine model for calculating the initial conditions of hydrolock in the Lotus Engine Simulation program

The calculation of the cycle was carried out taking into account heat exchange with the walls, which was ensured by setting the appropriate heat transfer coefficients in the

program (the program takes into account the heat exchange of gas between the walls of the combustion chamber and piston, as well as heat loss to the coolant).

Figure 3.8 shows calculated diagrams of pressure and temperature in the cylinder at modes from 1000 to 6000 rpm, including the selected mode of 3000 rpm [47]. This made it possible to set the initial pressure and temperature values that correspond to the moment the intake valves close. The data is necessary for subsequent modeling of hydrolock by calculating the compression stroke in the presence of liquid (for this example,  $p_0 = 0,123$  MPa,  $T_0 = 363$ K,  $\varphi = 220^\circ$ ).

It is characteristic that this method of selecting the initial values of pressure and temperature almost completely corresponds to the actual operating conditions of the internal combustion engine during hydrolock. That is, the cycle that precedes the liquid entering the cylinder is no different from normal and actually determines the initial conditions for hydrolock.

The accuracy of the results obtained and the possible error in the calculation of the compression process can be assessed. To do this, it is necessary to carry out a test calculation in the absence of liquid and compare the obtained values of pressure and temperature in the cylinder according to the proposed model with cycle data from the Lotus Engine Simulation program. Such a comparison is necessary, since the program provides a calculation of the complete closed cycle of an internal combustion engine, and the model provides only part of it.

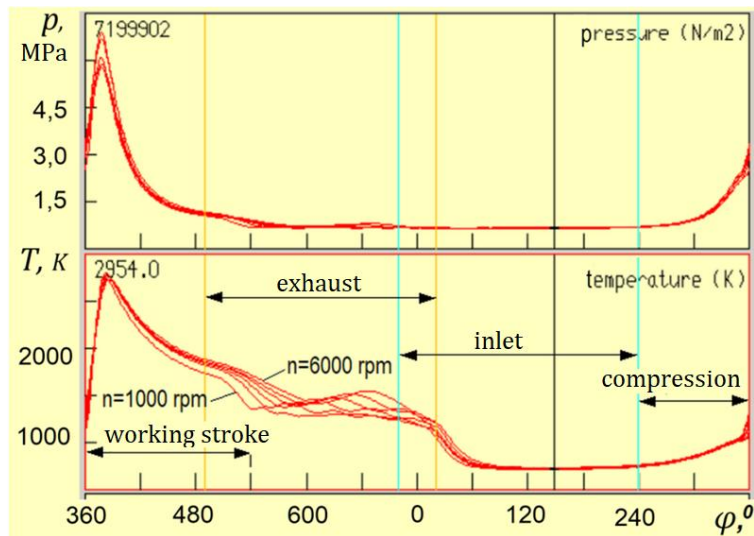
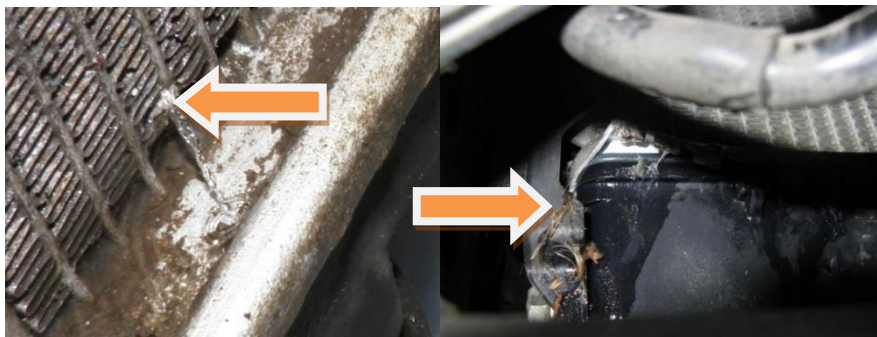


Fig.3.8. Diagrams of pressure  $p$  and temperature  $T$  in an internal combustion engine cylinder according to the crankshaft rotation angle  $\varphi$  at modes of 1000-6000 rpm, obtained using the Lotus Engine Simulation program [47]

## 4. LOCAL TEMPERATURE DAMAGE IN ENGINES

In operation, a large number of internal combustion engine failures are known due to an abnormally rapid coolant loss [35, 44]. The main cause of failures of this type is damage to the cooling radiator by various foreign objects from the road, thrown by passing or oncoming cars (Fig. 4.1). At the same time, there are often accidents with similar consequences associated with damage to hoses due to aging rubber (cracks, loosening of the clamps, tearing off the pipes).

All these damages and failures are local in nature, both at the location of the damage and in the development of the failure and the spread of damage only to some internal engine parts. Practice shows [35,90] that the engine with such damage fails due to loss of compression in the cylinders due to significant deformation of the mating planes and loss of tightness of the cylinder head gasket.



ab

Fig.4.1. Typical damage to radiators that cause rapid loss of coolant: a – in radiator tubes, b – in lower “can” (manifold)

Figure 4.2 shows the combustion chamber of a gasoline engine with traces of melting of the wall between the exhaust seats, which was the result of coolant leaking through the radiator, damaged by the impact of a foreign object. Such damage occurred when the engine was operating at nominal speed (the car was moving at high speed on the highway) and was characterized by high heating intensity and a short time before failure.

As might be expected, the area of the combustion chamber located between the exhaust valve seats received the greatest damage. This area is small, but it is heated by hot gases from 3 sides at once (combustion chamber and exhaust channels), while cooling is supplied only from one side.

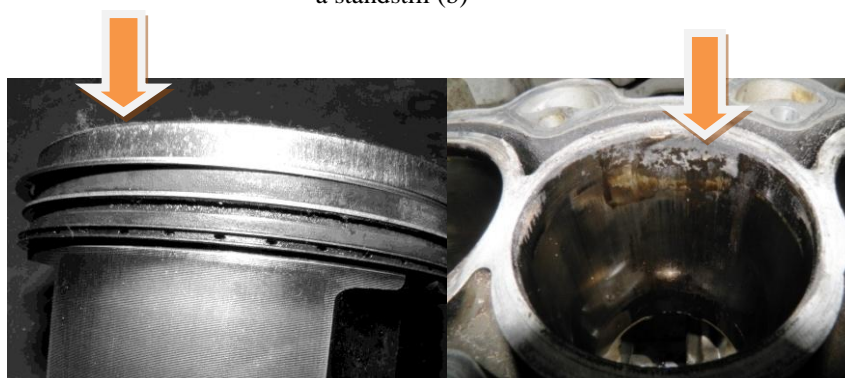
When operating at low speeds and loads, the heating intensity of parts decreases and the process time increases. This causes equalization of the temperature of the chamber wall,

and instead of a local burnout between the seats, engine failure is possible when the seat interference is lost due to thermal expansion of the materials (Fig. 4.3).



ab

Fig.4.2. A combustion chamber with traces of melting of the wall between the exhaust valve seats, damaged during the nominal operating mode of the internal combustion engine in motion (a), and a case of overheating with seats falling out due to loss of coolant at low speeds and loads when the internal combustion engine is operating at a standstill (b)



ab

Fig.4.3. Seizures on the upper part of the piston (a) and cylinder (b) of a gasoline engine due to coolant loss [35]

What is common in the two cases considered is minimal damage to the cylinders and pistons only in the upper part, where, due to thermal expansion of the bottom, the piston can jam in the cylinder with characteristic marks of scuffing (Fig. 4.3b).

Similar damage is possible in diesel engines. Thus, in an old prechamber diesel engine, with a rapid loss of coolant when the car was moving at high speed, the wall

between the prechamber and the exhaust valve seat burned out (Fig. 4.4), then another burnout occurred in the area between the cylinders due to its overheating, caused by a burnout of the cylinder head gasket.

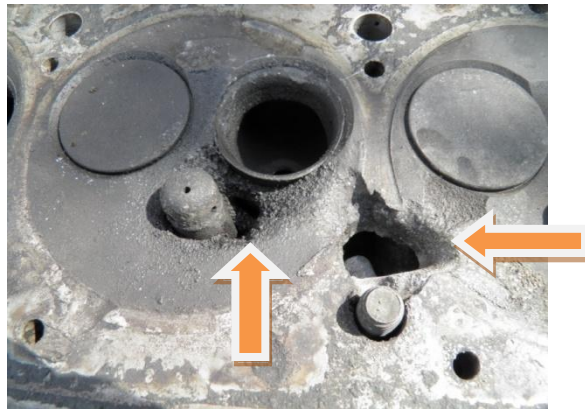


Fig.4.4. Melting of a diesel engine cylinder head due to overheating caused by sudden loss of coolant [35]

Moreover, even despite significant damage to the parts, the general trend remains the same. I.e. in the event of emergency overheating from coolant loss, the piston is damaged mainly in the upper area (Fig. 4.3), while the skirt does not have visible serious damage.



ab

Fig.4.5. Seizures in the upper part of the piston (a) and on the cylinder (b) from diesel overheating due to loss of coolant. The traces of gas breakthrough on the upper cylinder block surface are clearly visible [35]

These practical examples show good qualitative corresponding with the calculation data and confirm the theoretical result that during overheating from loss of coolant, damage to the combustion chamber is maximal and damage to the piston is minimal.

Common to the failure cases under consideration is the driver's lack of response to overheating and continuation of the trip until the engine emergency stops, which indirectly indicates the inoperability of the temperature sensor if it is installed on the outlet coolant pipe of the cylinder head (Fig. 4.6). This may be important when investigating the failure cause in order to conclude whether the driver could have recognized the occurrence of a malfunction in time and taken appropriate measures to prevent engine failure.



Fig.4.6. Features of the engine design (a, b – location of the temperature sensor on the outlet coolant pipe of the cylinder head), causing the temperature sensor to fail to respond to overheating in the event of an emergency loss of coolant [35]

So, if an emergency fault occurs in the cooling system, possible scenarios may be as follows:

- 1) the temperature control system worked normally and showed overheating, but the driver did not notice its readings and continued driving,
- 2) the temperature control system did not work and/or did not indicate overheating, as a result of which, the driver did not see it and also continued driving.

It is possible to determine how the processes of cooling failure and damage to parts occurred over time only through modeling [91].

However, the local nature of damage when the thermal regime is broken is not limited to the cylinder-piston group. The selective (local) nature of the damage was identified in practice when studying the failure in gasoline engines with variable valve timing [92, 93]. An example is a new 3.2litres V-6 engine that failed after only a few hours of early operation due to loss of compression in several cylinders [35]. Moreover, the

manifestation of the failure was associated with the activation of a diagnostic signal about problems in the valve timing control mechanism, caused by the lack of switching to wider intake phases when the rotation speed increases.

When investigating the failure cause, it was found that in some cylinders one of the two intake valves received a characteristic deformed tulip-shaped head [92] with obvious signs of overheating (Fig. 4.7). At the same time, no signs of damage were found on the intake valves located next to the damaged ones in the same cylinder. There was also no damage to the exhaust valves or their seats.



ab

Fig.4.7. Deformation of the head of one of the intake valves (a) in the form of a classic“tulip” (b) with complete absence of damage to the adjacent intake valve in the same cylinder (a). The case does not have a clear explanation within the traditional list of causes given for thermal overload of valves, including disruption of the combustion process

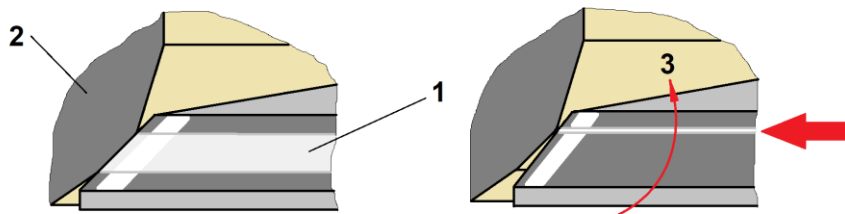
Among the existing signs of failure, should be noted the various stages of deformation of the intake valve head in different combustion chambers (Fig. 4.8), where it can be seen that the deformation of the valve head initially led to a change in the chamfer angle, making it inconsistent with the chamfer angle of the seat. This caused a sharp decrease in the width of the line of contact between the chamfer and the seat and its displacement to the inner edge of the chamfer.

It is clear that after even slight deformation of the valve head, the small width of the chamfer contact line along the inner edge of the seat becomes the cause of excessively high contact pressures and abnormally rapid wear of the valve chamfer with the formation of a characteristic narrow and deep groove (Fig. 4.8, 4.9).



ab

Fig.4.8. The deformation of the valve head caused displacement towards the inner edge and a significant reduction in the width of the contact area with the seat (a). With further operation of the internal combustion engine, this has led to severe wear of the chamfer and complete loss of contact with the seat (b)

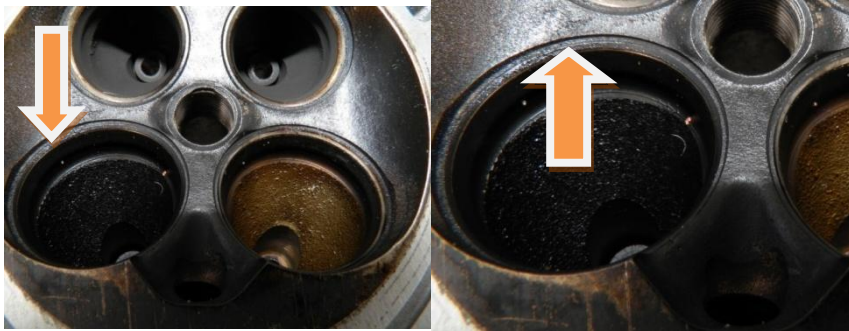


ab

Fig.4.9. Scheme of groove formation on the working face of the valve. Normal contact with the seat over a broad surface (a) in the case of tulip-shaped deformation turns into a narrow groove (b, marked with an arrow): 1 – valve head, 2 – seat, 3 – direction of deformation of the valve head relative to saddle touch lines

Further, due to the actual elongation of the valve from the deformation of its head and wear of the chamfer, a complete loss of the gaps (or the stroke of the hydraulic compensator plunger) in the valve drive mechanism occurs. Then the loss of contact of the valve chamfer with the seat occurs, during which overheating of the valve head, judging by its color in Fig. 4.7, becomes maximal.

A corresponding picture is observed in the combustion chambers (Fig. 4.10) next to the intake valve seats with a normal chamfer: there are traces of contact with the valves along the inner edge of the seats. Or without any traces of contact at all, when the valve has extreme elongening due to its head deformation and wear of the chamfer.



ab

Fig.4.10. Traces of abnormal contact of the intake valve with the inner edge of the seat (a) and almost complete absence of contact (b) as a sign of thermal deformation of the valve head

From the point of view of theory or practice, it is impossible to explain such selectivity of the overall effect of hot gases on only one intake valve in the absence of the same effect on all three other valves located nearby by some kind of combustion disorder. However, overheating of the intake valve head is also quite possible due to insufficient air cooling. At the same time, the cause of valve deformation, as well as the connection between deformation and overheating, as well as the local nature of the damage, are not entirely obvious and require clarification.

#### 4.1. Modeling the process of engine damage during an emergency coolant leak

In the case of faults associated with system leaks and external leakage, the pressure in the cooling system usually drops [35, 94, 95]. This causes the local coolant boiling on highly heated surfaces, which is dangerous for the engine, and the coolant release from the system expansion tank. For such cases, any traditional cooling system provides visual monitoring of the liquid level in the expansion tank. However, the emergency operation of a cooling system with a small amount of coolant in the system [90] differs significantly from “normal” overheating in the presence of coolant [96-97, 98-100]. One of the main differences is the dependence of the temperature state of the parts on the operating time under conditions of their non-stationary heating from hot gases when impaired cooling.

To analyze the operation of a cooling system with a low coolant level, it is necessary to take into account that a significant loss of liquid leads to a strong decrease in its level in the entire cooling system. This actually happens strictly according to the law of communicating vessels (Fig. 4.1), where the engine and radiator can be represented as two vessels connected by the lower pipe of the system [35].

Obviously, when the coolant level decreases, the system elements located at the highest points of the system will be exposed (that is, they will be left without liquid, or its

supply will not be continuous). According to the diagram of a traditional cooling system, at its upper level there are outlet pipes from the cylinder head to the radiator and interior heater. Therefore, the first external sign of a drop in the coolant level would be the heater turning off [35], clearly noticeable in the cold season.

For this mode, it is important that if the cooling system has a bypass channel between the cylinder head and the cylinder block, then the circulation of liquid in this channel will continue, since this channel is located below the cylinder head coolant outlet pipes (Fig. 4.11). When the coolant level is low, fluid can enter the upper part of the system only with a large pump flow, i.e. at high speeds. This means that in the cooling system in modes with low pump flow (at low and medium engine speeds), the main part of the liquid will circulate only through a small circulation circle.

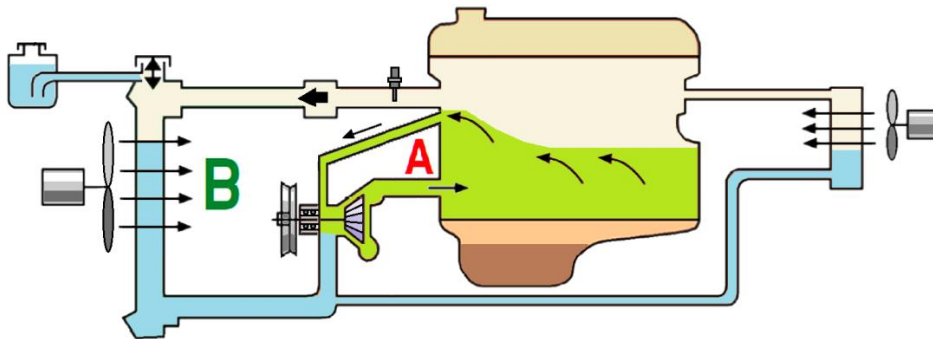


Fig.4.11. Scheme of operation of the cooling system during loss of coolant with continued circulation in a small circle

In this state of the system and in this operating mode, the radiator will be practically shut down as soon as the coolant level in the system drops below a certain critical value. This value may vary for different engines, but based on expert practice [35], usually a loss of 2-3 liters (or 30-40% of the total) will already be a critical loss for the system, provided the engine is operating at low and medium speeds.

It is typical that if there is a breakage in the supply or absence of coolant in the outlet coolant pipe of the cylinder head, the sensitive part of the temperature sensor located on the wall of the outlet pipe will actually be exposed. It means there may be a significant gap between the actual temperature and the temperature recorded by the sensor.

In order to more accurately establish the relationship between the heating of parts and the sensor readings in emergency mode, it is necessary to determine their change over time. To do this, it is necessary to find a solution to the task of unsteady heat transfer for the elements under consideration under the condition that their cooling is disrupted.

Let's imagine a certain element of the engine structure, heated on one side and cooled on the other (Fig. 4.12). When the engine is running, thermal equilibrium is established when the amount of heat transferred by the working fluid (gas) into the wall of the element is equal to the amount of heat transferred by the element to the coolant. In this case, a stationary heat transfer mode is implemented, and the temperature of the element will remain constant over time.

To the 1st approximation, thermal conductivity across the direction of heat propagation can be neglected, and the area of the wall through which the heat flow passes can be considered the same outside and inside. Then, for the specific heat flux  $q$  related to the cross-sectional area of the wall, one can use the equation [101, 102]:

$$q = \alpha_1 (T_1 - T_{w1}) = \frac{\lambda(T_{w1} - T_{w2})}{\delta} = \alpha_2 (T_{w2} - T_2) \tag{4.1}$$

where:  $\alpha_1$  is the heat transfer coefficient from the working medium to the wall,  $T_1$ ,  $T_2$  are the temperatures of the working medium and coolant, respectively,  $T_{w1}$  is the wall temperature on the heat supply side,  $T_{w2}$  is the wall temperature on the cooling side,  $\lambda$  is the thermal conductivity coefficient of the wall,  $\alpha_2$  is the coefficient heat transfer from the wall to the coolant.

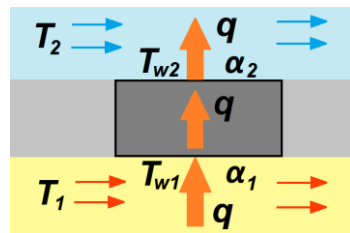


Fig.4.12. Design diagram of a cooled engine element

The specific heat flux from gas to liquid through the wall, taking into account the thermal conductivity of the wall, can also be written in general form according to the equation [101]

$$q = (T_1 - T_2) / \left( \frac{1}{\alpha_1} + \frac{\delta}{\lambda} + \frac{1}{\alpha_2} \right), \tag{4.2}$$

Now suppose that when operating in a steady state, wall cooling suddenly disappears as a result of a breakage of the coolant supply (we neglect heat removal with steam to the 1st approximation). This condition is equivalent to a sharp decrease in the heat transfer coefficient on the cooled side of the element, for example, as a result of an abrupt disappearance of the coolant (Fig. 4.13). In this case, the equilibrium between the heat

supply and removal is broken, therefore the equation (4.2), written for stationary heat transfer, cannot be used to calculate the temperature change in this process.

To approximately solve the problem of heating an element when cooling is broken, we will use the heat balance equation written for a selected element [101, 102] under the condition that there is no cooling:

$$q F d\tau = C_w M dT, \quad (4.3)$$

where  $F$  is the surface area of contact with the working medium,  $C_w$  is the specific heat capacity of the metal,  $M$  is the mass of the element,  $d\tau$  is the period of time during which the temperature of the element  $T_w$  increases by the amount  $dT$ .

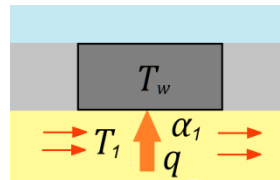


Fig.4.13. Design diagram of an engine element in case of cooling failure

Equation (4.3) shows the increase in the internal energy of a selected element when heat is supplied to it for a given period of time and there is no external cooling (including thermal conductivity across the heat flow).

Then from equations (4.3) and (4.1), under the condition that the cooling of the element is broken, we obtain a 1st order differential equation for the temperature of the element:

$$\frac{dT_w}{d\tau} = \frac{\alpha_1 F}{C_w M} (T_1 - T_w). \quad (4.4)$$

Equation (4.4) is a mathematical model that approximately describes the process of unsteady heat transfer, as a result of which the temperature of an element changes over time after an instantaneous breakage of its cooling. This corresponds to the emergency mode of operation of the cooling system with a rapid loss of coolant, provided that the cooling of the element with steam is neglected. For different elements of the system, for which the area, mass, heat capacity and heat transfer coefficient are different, therefore, we can expect different rates of temperature change over time from the moment the cooling conditions of the element change.

The solution of equation (4.4), taking into account the dependence of the heat transfer coefficient on temperature, as well as the approximate nature of the calculations, is easiest to perform numerically. For this purpose, the Euler or Runge-Kutta numerical integration method is quite suitable, which is implemented using iterations of the form

(3.23). Taking into account the equation (4.4) for the rate of change of element temperature, Euler's method, for example, will give the expression:

$$T_w = T_w + \frac{\alpha_1 F}{C_w M} (T_1 - T_w) \Delta\tau. \quad (4.5)$$

Since it follows from equation (4.4) that over time the temperature of the structural element under consideration will tend to the temperature of the environment, upon reaching which the temperature of the element will not increase (the temperature increment per unit time will become equal to zero), the limit of the temperature of the element will be its equality to the temperature of the environment.

It is clear that the model does not fully correspond to real conditions. So, not the entire element is completely located in a high-temperature environment, some part of the element is fixed to the wall, or it itself forms part of the wall, near which a high-temperature environment flows, so there is always a heat sink from the element. In addition, the temperature of the medium itself during the heating of the element can change over time, which will also affect the rate of increase in the temperature of the element.

However, it is possible to estimate the limits where quite reliable calculation results using this method can be expected. If we consider the real values of temperatures  $T$  and  $T_w$ , then in the case of exposure of an aluminum structural element to high-temperature combustion products, it turns out that the initial temperature difference is significant, and after a slight increase in the temperature of the element, further heating leads to a loss of strength by the material and failure due to the element destruction. Therefore, the accuracy of the calculation is obviously higher, the closer the current moment in time is to the beginning of the process, and this stage is a purpose of the calculation.

As an example, consider the task of placing a small aluminum structural element with an initial temperature of 400K (127<sup>0</sup>C) into a combustion product stream with a temperature of 1600K (1327<sup>0</sup>C). If you specify in the 1st approximation the size of the element (10 mm), its shape (for example, a cube), the surface area of contact with the high temperature medium (one side of the cube) and the order of magnitude of the heat transfer coefficient for given flow conditions (10<sup>3</sup> W/(m<sup>2</sup>K)), you can calculate the curve heating of such an element in the absence of cooling (Fig. 4.14).

As follows from the calculation results, in the event of a sudden and complete failure of cooling, the chamber wall will begin to melt after about 20 seconds of engine operation. Since the calculation did not take into account all the influencing factors (thermal conductivity along the wall, heat removal from the wall into steam, etc.), it is possible that the actual process time will be slightly longer. But in any case, the time until the cylinder head wall melts in the absence of its cooling will be calculated in seconds. In this case, the word “melting” should be understood as any thermal damage to the wall. For example, it can be not only through holes, but also surface erosion or loosening of the valve seats, as well as general thermal damage to the cylinder head in the form of significant deformation of the mating plane.

According to the calculation results (Fig. 4.17), the driver will see an increase in temperature on the gauge to  $100^{\circ}\text{C}$  (373K) only after twice as long, that is, after 40 s, when the cylinder head is already damaged and the engine actually fails.

Figure 4.17 also shows that heating of the piston when the cooling of the cylinder is disrupted occurs much more slowly, and scuffing on the top of the piston should be expected at a time several times longer than the time of damage to the combustion chamber wall (approximately 95 s after the start of the overheating process). In practice, this will mean that if there is severe thermal damage to the cylinder head, the damage to the pistons may be less severe.

#### **4.4. Model of the temperature state of the valve head with changing modes by the valve timing control program**

During expert studies of the technical condition of engines, cases of overheating of the intake valve heads were noted, which resulted in deformation of the valve head and loss of tightness of the valve-seat interface, causing engine failure [35]. From the point of view of well-known theories [27, 66, 105, 109] and practical experience [44, 110, 111, 112-114], to explain the overheating of the intake valve and not the exhaust valve, especially if it is only one of the two intake valves in one cylinder, is almost impossible. For this purpose, a theoretical study was carried out, as a result of which a method for modeling failures of this type was proposed.

Before starting the study, it is necessary to find out how the design of the engine itself can affect the temperature state of the valves. This is important if the design uses a timing mechanism [93]. In this case, as an example, we consider a special cam mechanism for changing the intake timing (Fig. 4.18). It provides not only a change in lifting, but also the duration of the open state of the intake valves (intake phase).

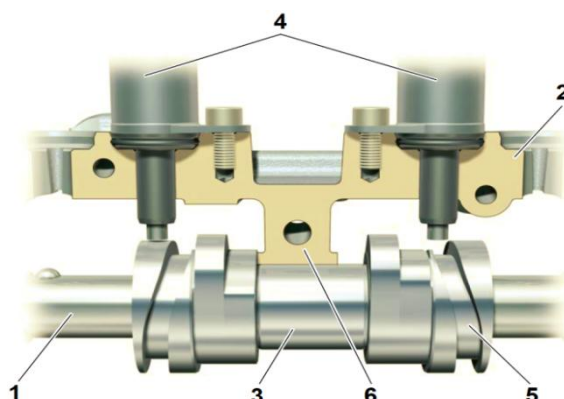


Fig.4.18. Structural diagram of the timing mechanism for changing the intake timing of the engine under study [93]: 1 – camshaft, 2 – housing, 3 – movable cam block mounted on splines, 4 – control electromagnets, 5 – groove for axial shift of the cam block, 6 – axial bearing

The specific design of the mechanism is of secondary importance in this case; more important is the program of regulation of the valve lift height and the duration of the open state of the intake valves. Thus, in the design under consideration, the control system maintains unchanged the lifting height and duration of the open position of one intake valve in each combustion chamber. At the same time, as the engine rotation speed and loading decrease, the lift height and duration of the open position of the second intake valve decrease.

To do this, by applying a pulse to the solenoid valves, the cam block on the camshaft is axially moved in one direction or another. This allows the second valve lifter to be switched to operate on a different cam profile. At the same time, the system corrects the intake timing to a later position, and the exhaust timing to an earlier position.

The change in valve timing is carried out stepwise according to the control program [93], in which both intake valves open simultaneously, but can close at different times depending on the engine operating mode (Fig. 4.19).

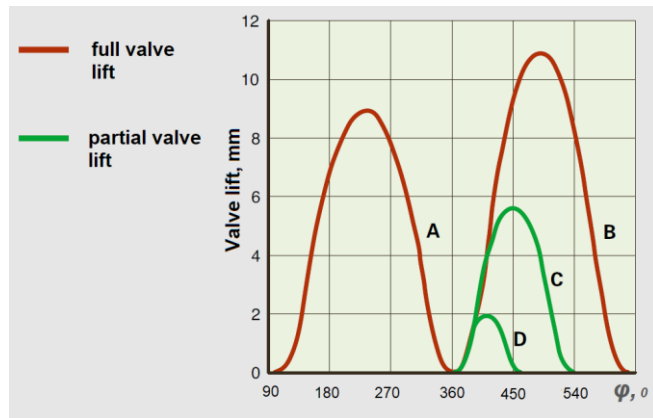


Fig. 4.19. The program for controlling the valve timing of the engine under study

According to the engine control program [93], switching from low lift and short duration of open state of the intake valves to large ones should be carried out with increasing speed and load. In case of system failure, i.e. if there is no switching, the corresponding fault code is recorded in the control system. From here it directly follows that in an engine with a similar valve timing control system, one should look for violations of the temperature state of the intake valves exactly where there is an anomaly in their operating mode. It especially concerns the case with low intake valve lift at increased speeds and loads.

To simulate the engine cycle with timing mechanism control [92, 115], the well-known Lotus Engine Simulation (LES) [62, 70, 71] program was used. The program is built on the so-called zero-dimensional model of the thermodynamic cycle of an internal combustion engine, for which cylinders and manifolds are elements of zero dimension. I.e. they have the properties of mass, pressure, temperature and volume, but do not have length. The conditions in these elements are calculated for each angle of rotation of the crankshaft by solving a system of differential equations for changing (incrementing) the pressure  $p$  and temperature  $T$  of the gas in the cylinder according to the angle of rotation  $\varphi$  of the crankshaft.

The purpose of the calculation when solving the task was not the main integral parameters of the engine (power, torque, specific fuel consumption), but this is the temperatures of the elements. Using the program, you can research a full multi-cylinder model close to a real engine, but a simplified 1-cylinder model is also quite suitable for the task of valve temperature state (Fig. 4.20).

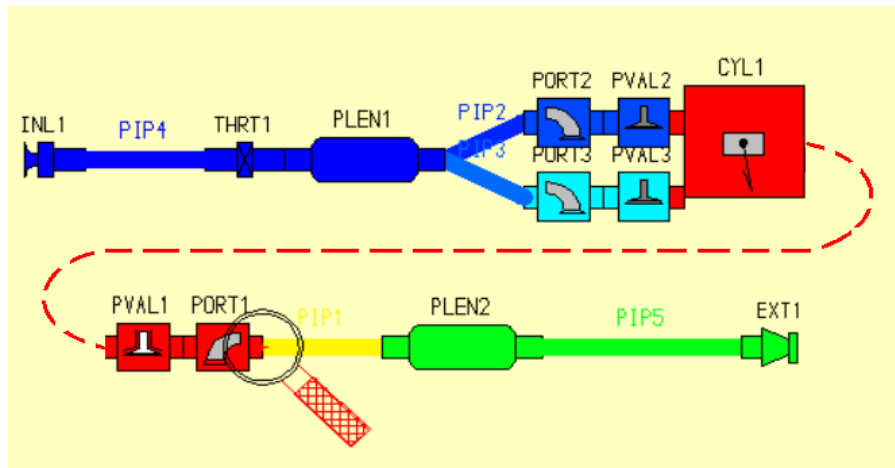


Fig. 4.20. 1-cylinder geometric engine model in the Lotus Engine Simulation program with the ability to set different lifts and timing for two intake valves [115]

To perform the cycle calculation, the actual dimensions of the engine cylinder and valve mechanism were specified. The engine model was built with two intake valves, which generally can have different control programs:

Type – gasoline, naturally aspirated

Working volume (for 4 cylinders) – 1700 cm<sup>3</sup>

Compression ratio – 10.5

Bore / stroke – 83 / 84 mm

Number of valves – 4 per cylinder

Valve head diameters (intake/exhaust) – 30 / 26 mm

Pipelines and manifolds were also chosen to be close to the real engine.

Cycle calculations were performed for rotation speeds of 1000-6000 rpm in increments of 1000 rpm at full load and 3 different intake valve timing options according to the control scheme given by the engine manufacturer (Fig. 4.21), in particular:

- 1) both intake valves open to the same maximum lift,
- 2) one valve has a 50% reduced lift and a 33% shorter duration of the open position (Fig. 4.21),
- 3) one valve has a minimum lift of 18% from the maximum and a 66% reduced duration of the open position.

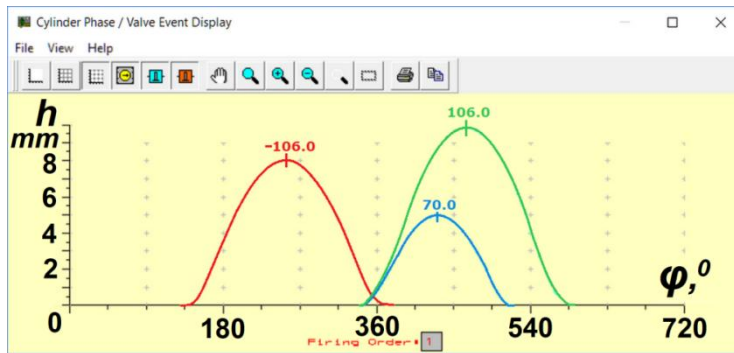


Fig. 4.21. Setting the valve timing for calculation: a variant with reduced lift and open duration of one of the intake valves is shown

At the same time, the general shift of the intake timing to a later direction, as well as the shift of the exhaust timing to an earlier one, was not specified to simplify the calculations. The reason is the lack of accurate data on the timing control program from the engine manufacturer.

The cycle calculation was carried out taking into account heat exchange with the walls. This is ensured by setting the appropriate heat transfer coefficients in the program (the program takes into account the heat exchange of gas between the walls of the combustion chamber and piston, as well as heat loss to the coolant).

The results of the cycle calculation were presented in the form of graphs of the dependence of the instantaneous parameters of air and gas in characteristic sections, including the cylinder and all pipelines (Fig. 4.22, 4.23). In addition, all instantaneous values of pressure, temperature and speed were saved in the form of Excel tables with a step of crankshaft rotation angle of  $2^\circ$ .

After obtaining data on the parameters for the cycle, a preliminary analysis of the calculation results was performed, including the presence of differences in the air flow near the intake valves.

It turned out that in the intake channel of a valve with less lift and opening duration, a significantly higher air temperature is observed with increasing rotation speed. This is obviously due to the reflux of gases from the cylinder into the intake channel at the initial moment of valve opening (Fig. 4.24).

It is clear that with a higher temperature of air (gases) in the section near the valve, a higher temperature in the valve itself should be expected. However, it is possible to determine the patterns of changes in the temperature of the intake valve when changing modes and valve timing using only thermal calculations.

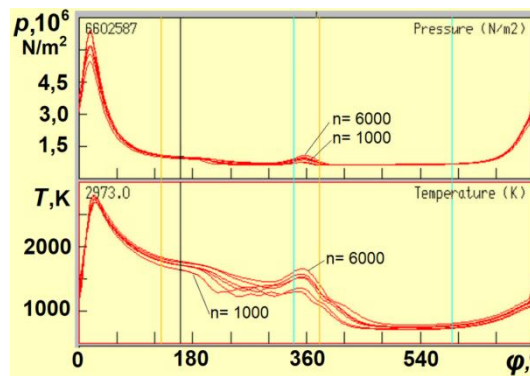


Fig. 4.22. Change in gas pressure and temperature in the cylinder according to the crankshaft rotation angle, obtained by calculation in the rotation speed range of 1000-6000 rpm for the case when both valves open synchronously

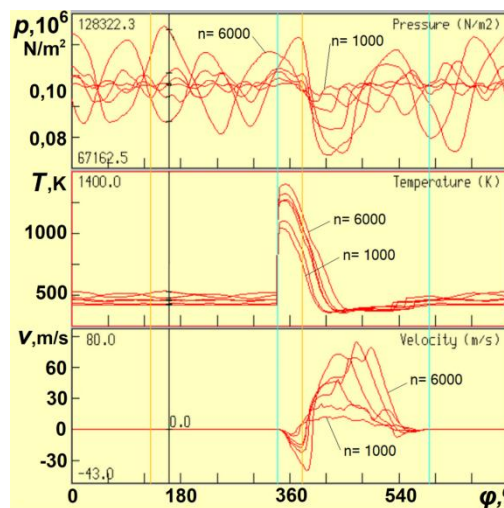


Fig. 4.23. Changing the instantaneous values of pressure, temperature and air velocity in the cross section of the intake pipeline in front of the intake valve in a cycle at different rotation speeds (both intake valves open synchronously)

## **5. LOCAL DAMAGE TO BEARINGS DUE TO ENGINE LUBRICATION SYSTEM FAILURE**

As is known, main and connecting rod bearings in internal combustion engines have different structural oil supply devices [19, 21, 35, 120-122]. Thus, the main bearings are lubricated with engine oil supplied to them from the engine sump by an oil pump under pressure from the main oil line in the cylinder block. At the same time, oil is supplied to the connecting rod bearings from the main bearings through radial-axial oil channels made in the crankshaft.

Damage to engine bearings is always or almost always local in nature, when some groups of bearings are damaged and others are not, and vice versa. The reason lies in differences in the lubrication conditions of different bearings, as well as in engine operating modes, especially after a failure in the lubrication system.

In the process of investigating the causes of malfunctions in the engine lubrication system, the following main and most common types of damage to crankshaft bearings are usually identified [44, 123, 124]. In accordance with manufacturers' data [125-127, 128-130], they can be divided into 3 main types:

1) most or all connecting rod bearings are damaged (Fig. 5.1). The damage is accompanied by the formation of traces of lubrication failure on the crankpins of the crankshaft, on the working surface of the bearings in the form of metal discoloration, scoring, melting and destruction of the bearing antifriction layer, with damage to the crank heads of the connecting rods. In this case, the main bearings show no signs of damage or they are insignificant,

2) most or all main bearings are damaged (Fig. 5.2). The damage is characterized by the formation of traces of lubrication failure on the main journals of the crankshaft, on the working surface of the bearings in the form of metal discoloration, scuffing, melting and destruction of the bearing antifriction layer, with damage to the crankshaft bearing holes in the cylinder block. In this case, the connecting rod bearings show no signs of damage or they are insignificant.

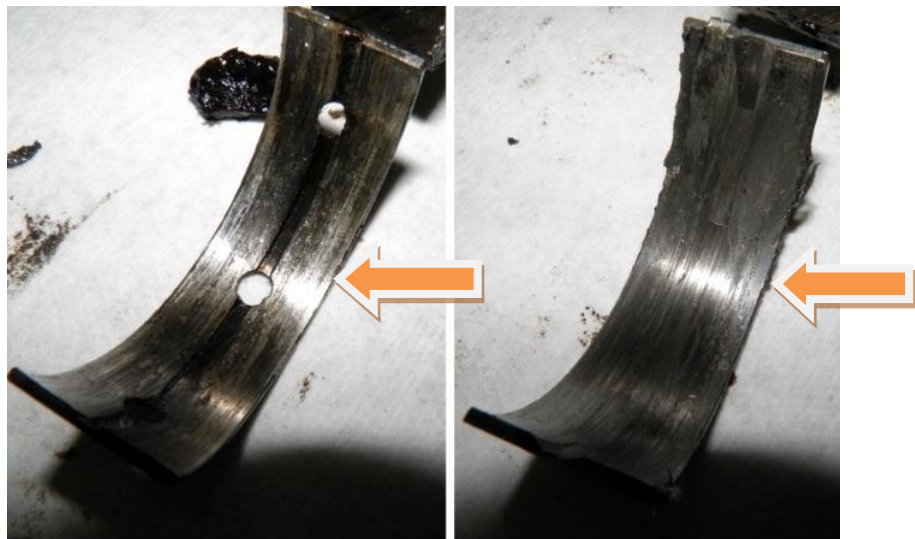
3) both the main and connecting rod bearings are damaged to one degree or another; they have damage traces of varying degrees (Fig. 5.3).

Based on the differences in the lubrication conditions of the connecting rod and main bearings, it is logical to assume that in the event of a sudden and complete cessation of oil supply to the crankshaft, lubrication failure will occur first in those bearings, where oil is supplied under pressure directly. Then the lubrication failure with a quick and complete breakage of oil supply should occur, first of all, in the crankshaft main bearings.



Fig.5.1. A typical example of damage to the connecting rod bearings (a) in the absence of noticeable damage to the main bearings (b) is a common result of operating an engine with insufficient oil levels

It also follows that the observed damage to only the connecting rod bearings (without damage to the main bearings) is possible not only in the case of a complete absence of oil in the lubrication holes of the crankshaft. Similar damage occurs when the oil supply is reduced, but not completely stopped (otherwise the main bearings would also be damaged).



a



b

Fig.5.2. The opposite case is damage to the main bearings through melting, jamming of the shaft and rotation of the bearings in the cylinder block (a). Damage to the main bearings was accompanied by relatively minor damage to the conrod bearings (b) and was caused by extremely rapid degradation of the engine oil with clogging of the oil receiver screen

Despite these obvious features of bearing damage, practice shows that some specialists, when determining the cause of such failures, do not take into account the observed difference in the degree of damage to the main and conrod bearings. As a result,

reports and conclusions indicate causes of lubrication failure that directly contradict the existing signs. At the same time, the presence of simultaneous damage to all crankshaft bearings causes the greatest difficulties in determining the reliable cause of the damage, corresponding to the real picture of engine failure.

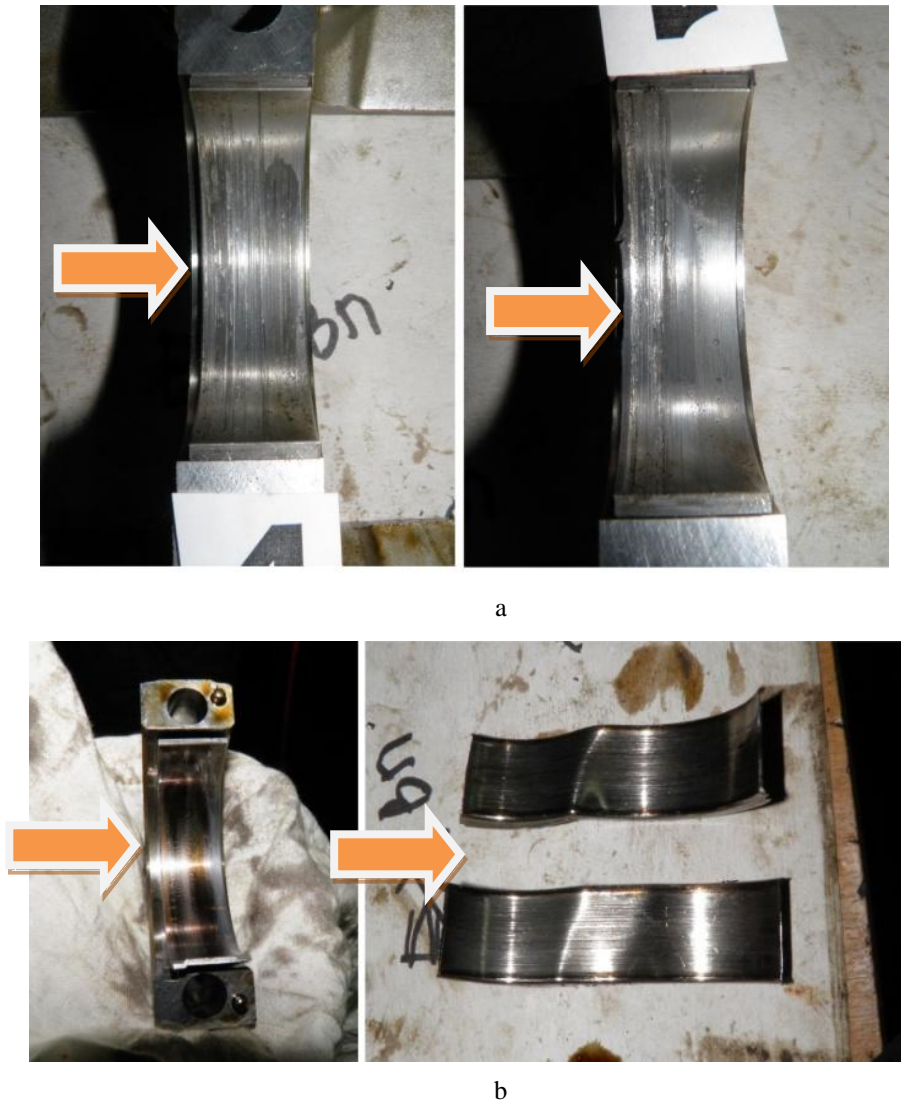


Fig.5.3. An example of damage to all bearings, both main (a) and connecting rod ones (b), as a result of long-term operation of the engine at high power modes with a faulty oil pump

In order to find out the cause why in some practical cases only one group of bearings is damaged, it is necessary to once again consider the well-known design scheme of internal combustion engine crankshaft bearings. Indeed, in the vast majority of automotive engine designs, main bearings, in addition to the main “bearing” function for the crankshaft, also serve as oil distributors for supplying oil to the conrod bearings. With the development of engine construction and as specific loads grew, a unified design scheme for main bearings was gradually developed [18, 20, 21, 35], which has the following distinctive features:

- 1) the lower half of the main bearing is made without an oil collection groove, which is necessary for maximum load capacity and minimal operational wear of the bearing,
- 2) the oil collection groove is made only on the less loaded upper half of the main bearing,
- 3) one or two holes are made in the crankshaft to supply oil from the oil collection groove to the conrod bearing.

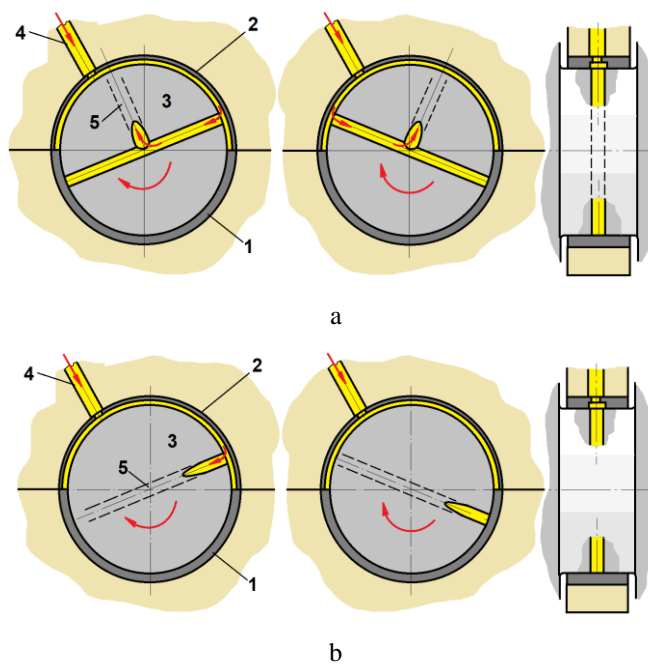


Fig.5.4. Structural diagrams of the main bearing: a – with a continuous oil supply through a transverse hole in the main journal, b – with an intermittent supply of oil through the hole connecting the main and conrod journals, 1 – lower half of main bearing without a groove, 2 – upper half of main bearing with a groove, 3 – crankshaft, 4 – oil supply channel to the main bearing, 5 – oil supply hole to the conrod journal

An analysis of the designs of automobile internal combustion engines produced at the end of the 20th and beginning of the 21st centuries shows that the holes in the crankshaft for supplying oil to the conrod bearings are made in 2 versions (Fig. 5.4):

- 1) the main journal is drilled through and across its diameter, then a hole is made in the crank journal until it connects with the hole in the main journal,
- 2) only one through hole is drilled, connecting the main and connecting rod journals.

It is easy to notice that the crankshaft can have only one hole in the main journals. If, in this case, there is an oil collection groove only on the upper halves of the bearings, an intermittent supply of oil to the conrod bearings occurs in the crankshaft lubrication hole.

Indeed, when the crankshaft rotates, the oil supply hole in the conrod bearings is open only those half turns when it coincides with the oil collection groove on the upper main bearing. The remaining half-turn, the hole is closed by the lower half of the bearing, and no oil is supplied to the lubrication hole to the conrod bearings. In this case, it is necessary to clarify how the conrod bearing operates without oil supply.

The answer lies in the very difference in the methods of supplying oil to the main and conrod bearings. Oil flows to the main bearings continuously and directly from the lubrication system of the oil pump. On the contrary, oil comes to the conrod bearings from the oil collection groove on the main bearings. In this case, the location of the conrod journal axis with a displacement to the crank radius (with eccentricity) from the main axis determines a significant difference in lubrication conditions. In fact, even when the lubrication hole in the crankshaft is completely blocked, the supply of oil to the conrod bearings inevitably continues, probably under the influence of centrifugal forces.

That is, judging by the available data [35, 121], not only the method of oil supply differs, but also the nature of damage to the main and conrod bearings. This suggests that the indicated difference is caused precisely by the influence of centrifugal forces. Therefore, let us consider in more detail how significant such an influence can be.

## 5.1. Evaluation of the centrifugal force influence on bearing lubrication

Let us first consider a simplified diagram of oil supply from the main journal to the conrod (Fig. 5.1), for which we will accept the following assumptions:

- 1) lubrication hole is drilled approximately along the radius of the crank,
- 2) engine oil flow in the hole has the property of continuity,
- 3) oil supply from the main bearing is shut off completely,
- 4) crankshaft rotates at a constant speed of 3000 rpm, which corresponds to medium engine speed mode.

Obviously, the oil pressure  $p_{oc}$  in the outlet section of the hole (on the connecting rod journal) under such conditions will be determined by the formula

$$P_{oc} = F_c / f \tag{5.1}$$

where  $f$  is the cross-sectional area of the hole,  $m^2$ , and the centrifugal force acting on the oil column in the hole is equal to

$$F_c = m_x v^2 / R. \tag{5.2}$$

This corresponds to the mass of the oil column

$$m_x = \rho f l_x \tag{5.3}$$

where  $\rho$  is the density of the oil ( $\rho = 900 \text{ kg/m}^3$ ),  $l_x$  is the length of the oil column affected by the unbalanced centrifugal force, m.

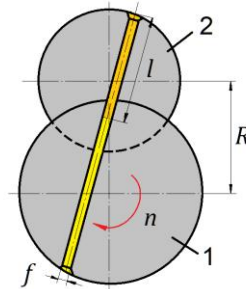


Fig.5.5. Simplified calculation diagram of oil supply from the main (1) to the conrod (2) crankshaft journal

Then from well-known expressions (5.1)-(5.3) we can obtain a formula for calculating oil pressure from centrifugal forces:

$$P_{oc} = \rho l R n^2 (\pi^2 / 900). \tag{5.4}$$

As follows from the diagram of the unit, the crank radius and the length of the oil column in the hole are approximately equal values, so for simplicity we equate them to each other. Then the formula for calculating the oil supply pressure in conrod bearings from centrifugal forces will receive the following simple final form:

$$P_{oc} = \rho R^2 n^2 (\pi^2 / 900). \tag{5.5}$$

If we take the average value of the crank radius to be 0,05 m, then the simplest calculation will give an approximate value of the oil supply pressure from centrifugal forces  $p_{oc} = 0.22 \text{ MPa}$  after failure of the oil supply to the main bearings.

Indeed, this result confirms cases known from practice of severe damage or even jamming of the main bearings in the absence of damage to the connecting rod bearings.

However, this theory cannot explain some features of the failure, for example, cases when all bearings are damaged, but to varying degrees, since it does not take into account the effect of engine operating time on the oil supply. For example, formula (5.5) does not take into account a number of factors important for practice, including, it does not make it possible to determine how long the lubrication of conrod bearings will remain after an oil supply breakage to the system. That is, it allows us to give only a preliminary, rather rough, qualitative assessment of the process under study.

## 5.2. Model of changes in oil supply pressure to bearings after oil system failure

For a more accurate evaluation of all factors affecting the supply of oil to the connecting rod bearings in emergency mode after a failure in the engine oil system, it is necessary to clarify the oil supply diagram from the crankshaft main journal to the conrod journal. To do this, consider a diagram that is as close as possible to the actual design of most crankshafts of modern automobile internal combustion engines (Fig. 5.6).

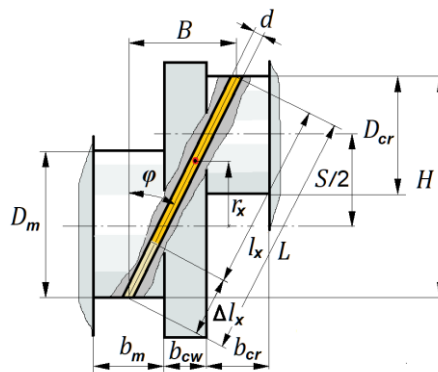


Fig.5.6. Detailed calculation diagram of oil supply from the main journal to the conrod journal

The main purpose of the calculation can be formulated as determining the change in pressure in the lubrication hole in front of the conrod bearing after failure of oil supply to the main oil channel (in front of the main bearing). To solve this, it is necessary to find the mass of the oil column in the lubrication hole and the coordination of its center of mass. This will allow us to calculate not only the pressure in the area of the lubrication hole on the conrod bearing, but also the change in this pressure over time.

From Fig. 5.6, obvious geometric relationships for the axial width  $B$  of the lubrication hole follow:

## **6. EXPERIMENTAL RESEARCH OF PERFORMANCE FAILURES IN AUTOMOTIVE INTERNAL COMBUSTION ENGINES**

### **6.1. Statistic analysis of performance failures in automotive internal combustion engines**

The sufficient increase of the number of automobile transport aggravates the topicality of the issue of increasing road trains' operational reliability. Due to this, the important role belongs to the interconnection of reliability theory and technical operation of vehicles defining directions and methods of the research in the area of operational reliability of the vehicles. One of the characteristic indexes of the reliability theory are random values having drift even under the steady conditions of obtaining results, and furthermore, in the area of operation of vehicles: transport flow on the roads, appearance of failures and malfunctions, time and labour intensity of their removal, preventive effects etc.

The research of the given facts and regularities provides: making a qualified decision of calculations with the usage of the mathematical apparatus; not accounting a random character of process of rolling stock technical operation, but the research and usage of the obtained regularities in practice.

The methodology of researching random laws of random values distribution during technical exploitation comes down to the combination of experimental data description with the help of these or other laws of distribution with the construction of mathematical models of researched processes that is proven by the founders of the theory of probabilities such as Pascal, Fermat, Bernoulli. They were "convinced that distinct regularities may occur based on massive random events" [134, 135].

Resulting numerous research, it was established that the laws of distribution that occur the most frequently during description of random values in technical operation of cars are normal, Weibull, logarithmically normal, exponential laws of distribution.

At the same time, the common tendency, explaining the increase of variation index, implies gradual and increasing violation of central limit theorem of A.M.Liapunov, consisting in the appearance of outlier factor in influence while summing up the sequence of random factors or in the non-sufficient deviation from the function of altering the parameter according to the time (mileage) from the linear, or, depending on the intensity of random factors influence from the level reached by the random value [136, 137]. However, the stated models, though they are not typical, however, they do not exclude the occurrence of the new ones, for a more complete description of a wide class of the processes, characteristic to the technical exploitation of the automobiles.

Using the principles of program-targeted approach and analyzing the fulfilled works as for the vehicles' operational reliability, it was formulated the key tasks of researching of the combustion engines' operational reliability:

- to detect efficiency violation of internal combustion engines;
- to determine the least reliable joints and parts under the operational conditions;
- research of regularities of occurring failures and deviations of performance;
- determining time consumption for detected defects removal;
- spare parts nomenclature formation at automobile transport enterprises;
- engine coupling wear assessment.

The examination comprised the new truck tractors as part of road trains with semi-trailers during the warranty and post-warranty operating periods. Maintenance of the vehicles was conducted according to the recommendations of manufacturing plants. The road trains are exploited on the roads of the I-st and the II-nd categories of exploitation conditions.

The aim of the work was the research of regularities of occurring failures and deviations of performance, determining time consumption for detected defects removal.

The methodology of solving the tasks of initial data processing as for the vehicles' reliability included the processes of obtaining and processing the data. The methodology consists of the two blocks: 1 – collecting data as for performance reliability and their systematization; 2 – the statistic processing for determining parameters and types of distribution laws; 3 – determining parameters of general aggregate; 4 – draw of conclusions and suggestions.

Block 1 consists of the three groups. Statistical data undergo a thorough analysis, having organized the sampling of truck tractors' one model, of one year of manufacture, with equal features of limit states.

Depending on the sampling type, a further specialization of calculation operations is conducted. It is provided character determination (random – non-random) of outstanding observations for the complete samplings (Block 2); determining the laws of distribution (check-up according to the agreement criteria).

Block 3 comprises parametric and non-parametric ways of samplings comparison. Parametric ways are spread on the medium values of dispersion, that is on statistics. Non-parametric ways presuppose the values of all members of dispersion (variants) of the compared samplings, that is the presence of the initial information. If it turns out that that according to the selected criteria of assessment, samplings do not belong to none of the general aggregate, it is necessary to check the results obtained before. Therefore, the methodology implies reverse connections (feedbacks).

Block 4 implies obtaining conclusions and suggestions regarding the improvement of the construction (modernization) or technical maintenance technology.

### 6.1.1. Warranty operation period

Basing on the collected data regarding the research of defects and malfunctions of the control groups of the new 50 truck tractors (Group 1) and 100 truck tractors (Group 2) diagrams of accumulated frequencies, distribution of mileage before the appearance of cars malfunctions, distribution of malfunctions by aggregates, nodes, mechanisms and systems were constructed [138].

During the warranty period of operation, the appearance of malfunctioning vehicles of group 1 is well approximated by the beta distribution (Fig. 6.1) with statistical characteristics for an engine with a failure probability of  $P_i=0.099$ : mathematical expectation  $M - 49,252$  thousand. km; variance  $D - 222,376$  thousand km;  $\sigma$  mean square deviation - 14,912 thousand km; coefficient of asymmetry  $\gamma_1=-0.537$ ; coefficient of excess  $\gamma_2=-0.399$ ; (Fig. 6.2).

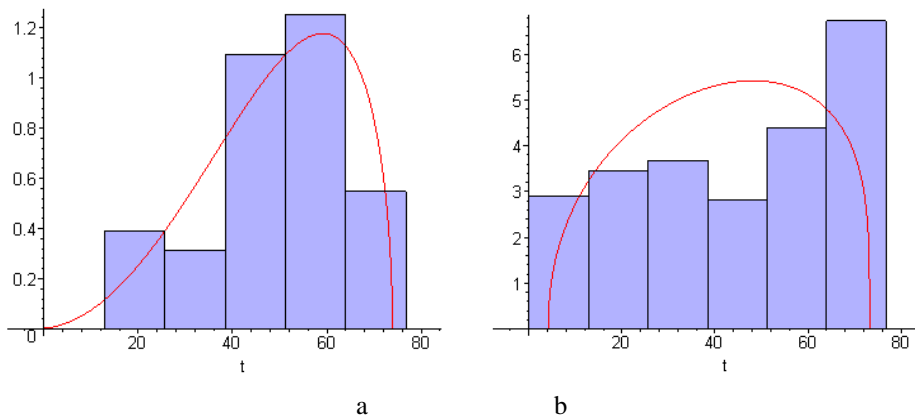


Fig. 6.1. Bar charts and theoretical curves of the distribution of group 1 malfunctioning vehicles of: a – engine; b – aggregates; c – autonomous heater; d – other; e - electrical equipment; f –fastening connections violation

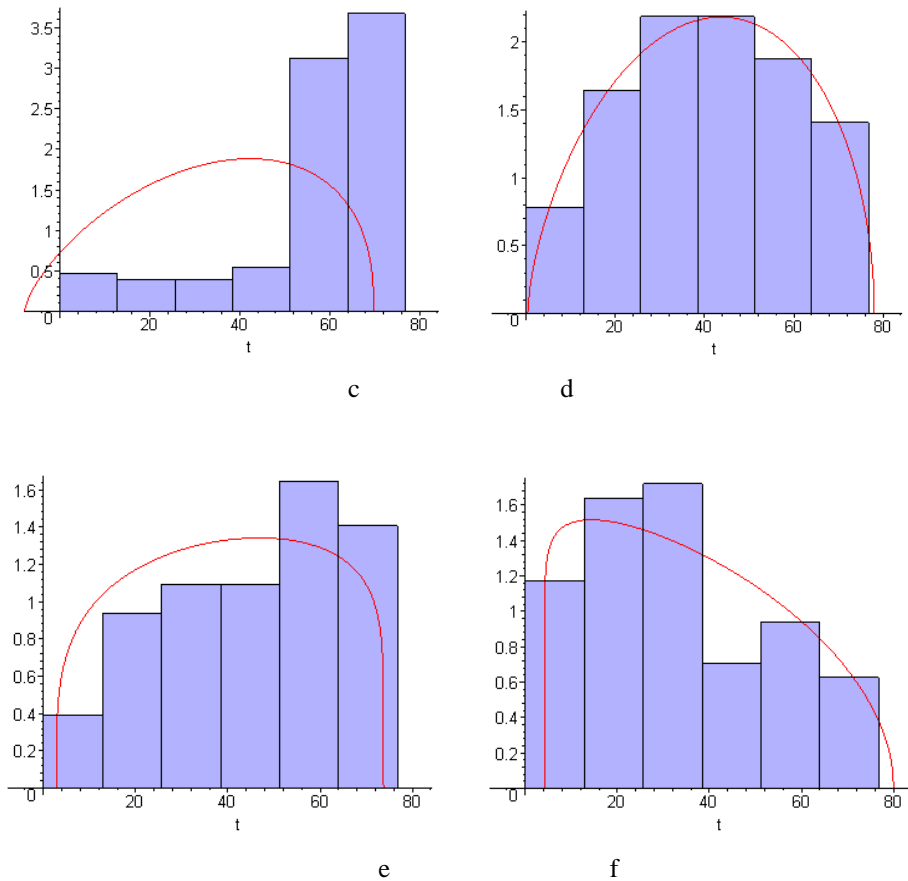


Fig. 6.1. Bar charts and theoretical curves of the distribution of group 1 malfunctioning vehicles of: a – engine; b – aggregates; c – autonomous heater; d – other; e – electrical equipment; f – fastening connections violation

The first year of operation, the appearance of group 2 vehicles malfunctioning is also approximated by the beta distribution (Fig. 6.3) with statistical characteristics for the engine with a failure probability of  $P_i=0.066$  (exponential law of distribution): mathematical expectation  $M - 1.4$  thousand. km;  $\sigma$  mean square deviation – 0.8 thousand km (Fig. 6.4).

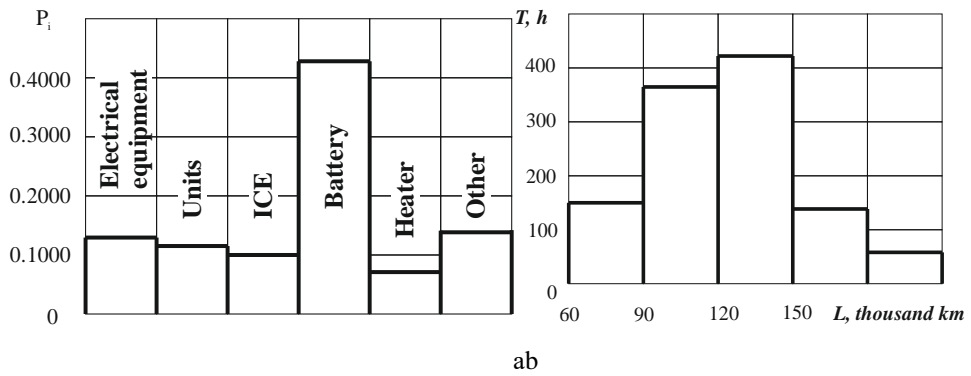


Fig. 6.2.Characteristics of group 1 vehicles malfunctioning: a – distribution of mechanisms and systems malfunctions; b – recovery time distribution

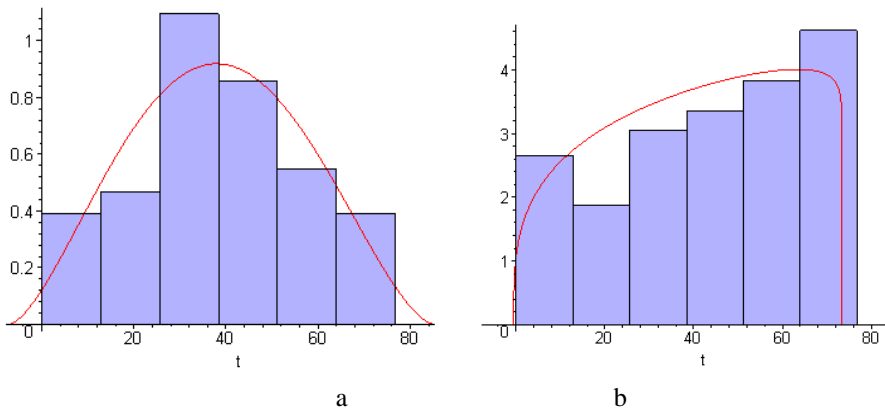


Fig. 6.3. Bar charts and theoretical curves of impaired performance of group 2 vehicles distribution: a – aggregates; b – suspension; c – steering; d – electrical equipment; d – oil seal of the main transmission leading gear; e – fastening connections weakening

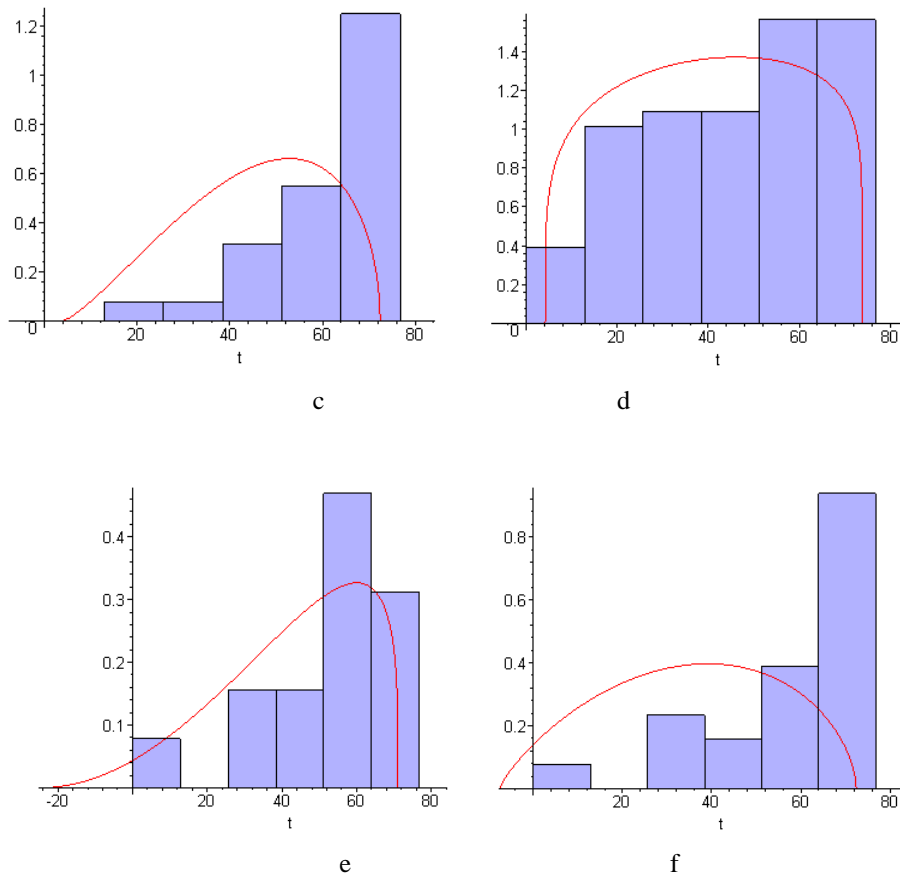


Fig. 6.3. Bar charts and theoretical curves of impaired performance of group 2 vehicles distribution: a – aggregates; b – suspension; c – steering; d – electrical equipment; d – oil seal of the main transmission leading gear; e – fastening connections weakening

Classifying violations of the vehicles' performance according to external signs, it was established that most of them relate to breakage, loosening fasteners and wear. The specific weight of failures due to wear was about 20%. The study of the distribution laws of work per failure during the operation warranty period shows that there are symmetric, but in a larger number - asymmetric distributions. Knowledge of the patterns of failures occurrence allows solving practical problems in the spheres of automobile production and their operation.

Symmetrical laws of the distribution of maintenance on failure, as a rule, indicate the perfection of the design, and an increase in maintenance can be achieved by improving the modes and technology of maintenance and fixing. This information can be used in operation to determine the scope of repair actions to eliminate the corresponding failures.

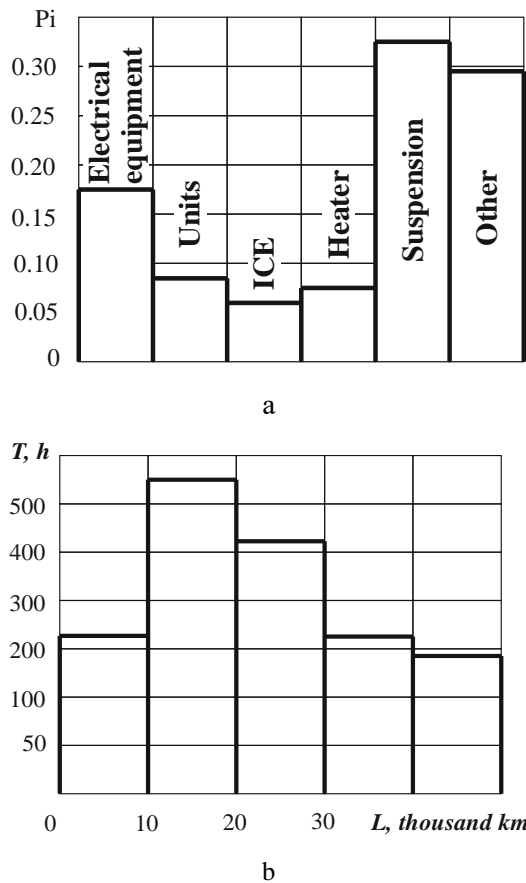


Fig. 6.4. Characteristic of group 2 vehicles malfunctioning:  
 a – distribution of mechanisms and systems malfunctions;  
 b – recovery time distribution

Asymmetrical laws of distribution in some cases indicate deficiencies in the design or technology of their assembly or unqualified driving the vehicle. The study of these laws made it possible to gain a deeper understanding of the failures nature, their physical essence, to develop a strategy for their prevention, to model and predict violations of the vehicles' technical condition.

The completed reliability assessment during the warranty period of the vehicles' operation made it possible to identify the least reliable components that need to be improved in design and manufacturing quality. The conducted analysis of the defects elimination made it possible to distribute them by work type into four groups: replacement of parts and assemblies (57.5%), adjustment work (22.9%), fastening work (10.1%), diagnostic work (9.5%). The main regularities are shown in fig. 6.5.

The stay of cars under repair with a short time for troubleshooting (up to 2 hours and from 2 to 4 hours) was 7.8% and 7.6%, respectively; 22.2% were car downtimes during troubleshooting from 4 to 8 hours; 62.4% were idle vehicles with more than 8 hours of troubleshooting time.

The analysis of vehicles' downtime during warranty repairs showed that the average duration of one repair is 13.7 hours. It was established that after 60 thousand km mileage stabilization stops and at a mileage of more than 100 thousand km, the average idle time is 20.2 hours.

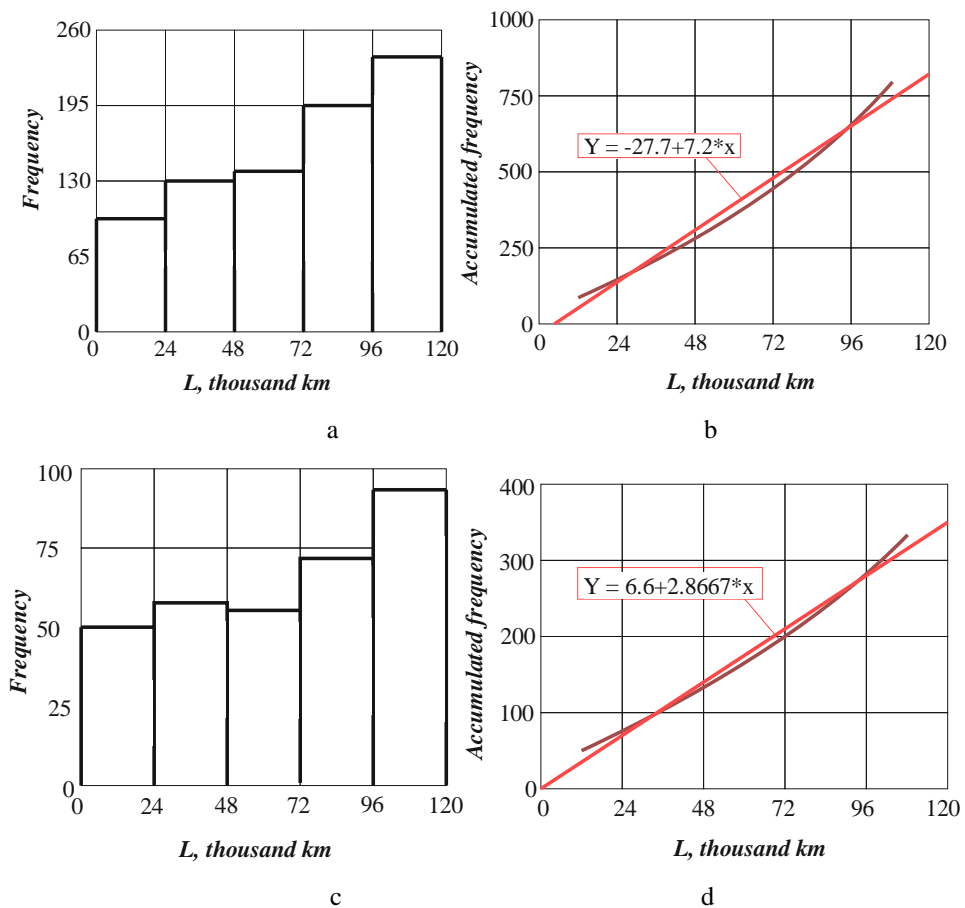
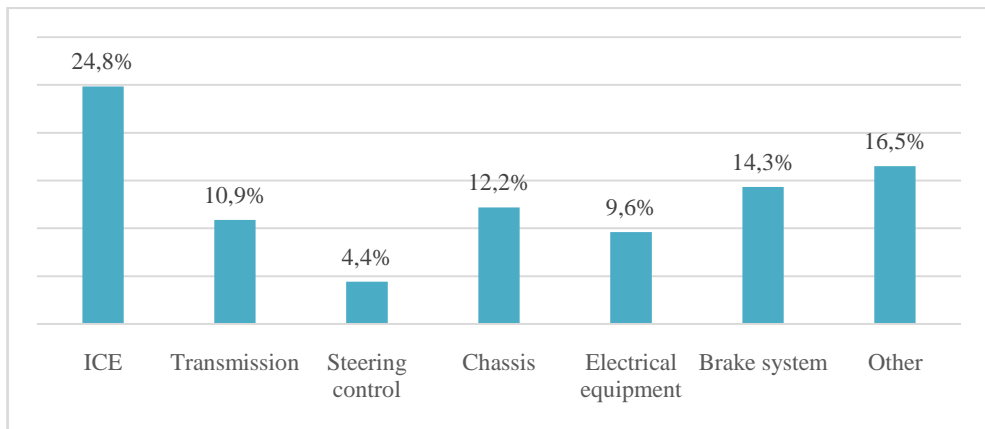


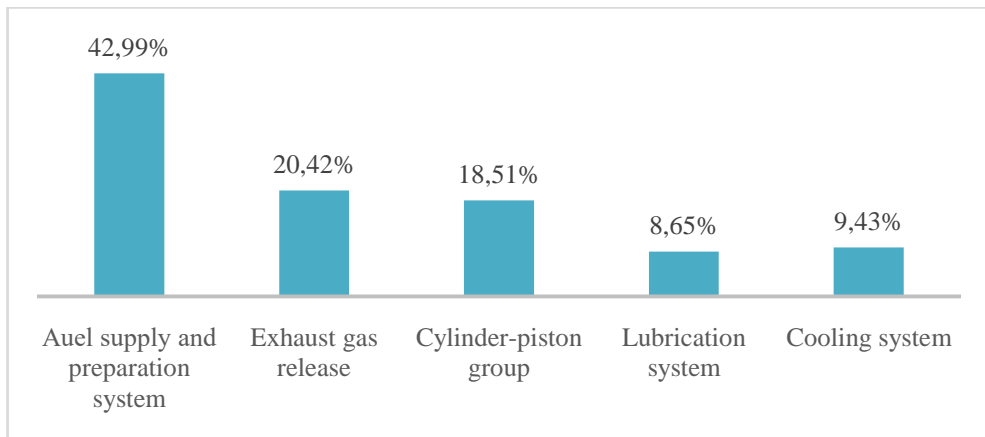
Fig. 6.5. Frequency (a, c) and accumulated frequency (b, d) of applications (a, b) for warranty repair and warranty repair (c, d)

**6.1.2. Post-warranty operation period**

The analysis of malfunctions of 100 Group 1 vehicles in the post-warranty period of operation (10 years of observation, the average mileage of one car is 858.42 thousand km) showed that the following malfunctions of the motor (24.84%), transmissions, failures or violations working of the undercarriage, malfunctions of the heating system and cabin lifting are often found (Fig. 6.6 a). The distribution of the total number of replacements on cars obeys the normal law of distribution (table 6.1). The average number of refusals per car was 13.29; average mileage before the first failure – 141,750 km; average mileage before failure – 40,598 km [139, 140].



a



b

Fig. 6.6. Characteristics of malfunctioning vehicles of group 1 in the post-warranty period of operation: a – vehicles malfunctioning; b – engine systems malfunctions

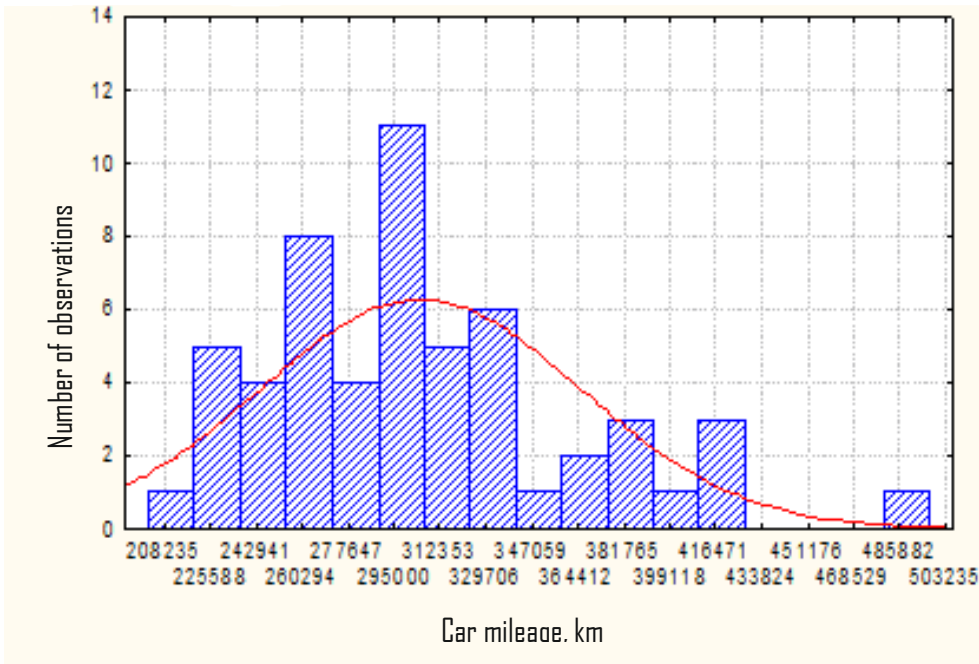
Table 6.1. Statistical data characteristics

Variable	Distribution type	Probability density
General distribution	Normal	$f(x) = \frac{1}{89837.23\sqrt{2\pi}} e^{-\frac{(x-302008.3)^2}{2 \cdot 89837.23^2}}$
Head of the cylinder block	Normal	$f(x) = \frac{1}{60812.02\sqrt{2\pi}} e^{-\frac{(x-304836.4)^2}{2 \cdot 60812.02^2}}$
Muffler elements	Uniform	$f(x) = \begin{cases} \frac{1}{325000}, & x \in [77000; 401000], \\ 0, & x \in [77000; 401000] \end{cases}$
Set of gaskets	Normal	$f(x) = \frac{1}{71886.01\sqrt{2\pi}} e^{-\frac{(x-322957.6)^2}{2 \cdot 71886.01^2}}$
Adblue nozzle	Uniform	$f(x) = \begin{cases} \frac{1}{338000}, & x \in [85000; 413000], \\ 0, & x \in [85000; 413000] \end{cases}$

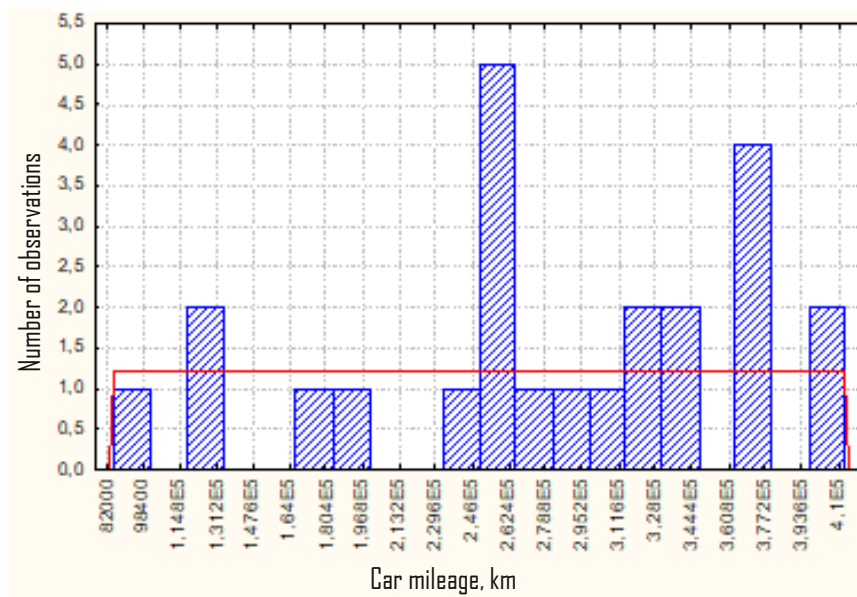
Analyzing malfunctions of engine systems (Fig. 6.6 b), which are basically every fourth malfunction, it can be noted that 42.99% are malfunctions of the fuel mixture supply and preparation system (replacement of nozzles, their cups and seals, repairs of the moisture separator). Most of the malfunctions of the exhaust gas system consist of muffler corrugations, replacement of exhaust manifold gaskets replacement. In the cylinder-piston group, the main and connecting rod bushings were changed during the operation period, the rear oil seals of the main bearing turned out to be the weak point; in the cooling system - a thermostat. Replacements in the lubrication system are characterized by failure of the oil pressure sensor (table 6.2). The characteristics of some engine elements impaired performance are shown in Figure 6.7. Examples of malfunctioning engine components are shown in Figure 6.8.

Table 6.2. Distribution of performance according to engine elements

Unit elements	Failures, %	Performance until the first failure, km	Average performance until failure
Head of the cylinder block	11.4	202000	304836
Muffler elements	11.4	77000	237927
Adblue pump	3.9	105000	515368
Cooling system pump	1.0	312000	391000
Fan drive hub	0.6	192000	286333
Accelerator rheostat	1.9	45000	206333
Thermostat	3.1	145000	296733
Flywheel bearing	1.2	291000	356333
Set of gaskets	48.8	202000	322958
Turbine	0.2	196000	196000
Intercooler pipe	0.2	447000	447000
Radiator	0.2	283000	283000
Adblue nozzle	5.0	85000	280042
Adblue external filter heating	4.1	105000	360700
Fan belt	0.2	410000	410000
Distribution shaft	0.2	389000	389000
Adbluehoze	2.1	42000	284100
Oil pressure sensor	0.8	95000	148750
Crankcase gas sensor	3.7	65000	245278



a



b

Fig. 6.7. Characteristic of the cylinder head (a) and Adblue nozzles (b) malfunctions



a



b



c



d



f

Fig. 6.8. Examples of engine elements malfunctions:  
a, b, c – failure of the valve spring and its consequences;  
d – thermostat; f – Adblue pump

## CONCLUSION

The study was the first to show that the durability of an internal combustion engine may depend not only on the efficiency of air filtration and wear resistance of parts, but also on the design of the engine intake system.

The developed model of a 2-phase flow of air with dust in the intake channels describes and explains the mechanism of the occurrence and development of a malfunction for certain types of operational damage. The model helps to determine the cause of the uneven local abrasive wear of parts of the cylinder-piston group and valve mechanism observed in practice in individual internal combustion engine cylinders, when more than 85% of incoming particles are locally concentrated directly downstream. The models built based on the description of the movement of a single particle and using the finite volume method implemented in the ANSYS program make it possible to explain this redistribution of dust particles in the intake manifold. This effect corresponds to the data of expert studies, when, due to the centrifugation of dust into the farthest channel of the intake system, the engine life can be reduced several times even with the air filter in normal condition.

The simulation results show that due to the inevitable entry of abrasive particles into the intake system, calculation models based on the "clean" air hypothesis miss the centrifugation and redistribution of abrasive particles in the branching inlet channels. On the contrary, it is necessary to take into account the redistribution of particles along the channels of the intake system is necessary both when designing new and when upgrading existing engines, in order to clarify the regulations for their maintenance, in order to prevent a sharp decrease in durability due to local abrasive wear. Based on the data obtained, the main design and operational methods are indicated to reduce the particle redistribution and eliminate local abrasive wear.

In addition, the study has found that local abrasive wear is actually another wear mechanism, which depends on the number and size of particles passing through the air filter, the configuration of the intake system and engine operating conditions. This feature of the impact of particles must be taken into account when conducting expert studies of the engine technical condition in order to correctly determine the failure causes associated with breakage of operating conditions.

By using the standard Lotus Engine Simulation software to calculate the internal combustion engine cycle, the models of local damage to parts of the conrod piston group during compression of air with liquid and of deformation of the connecting rod stem in a hydraulic lock were developed. As a result of this work, the dependence of the value of deformation of the connecting rod on the combustion chamber liquid filling factor was obtained. By calculation, using the finite element method in the ANSYS program, the stress-strain state was simulated. The previously missing data that deformation of the connecting rod with loss of stability of the stem occurs when the combustion chamber is filled with liquid to a minimum of 80% was obtained. This corresponds to an axial

deformation of the conrod stem of about 0,5 mm. With further compression, the longitudinal bending of the stem increases multiple times and amounts to twice the axial deformation. Further, with an increase in the amount of liquid within the limits of up to 110% of the volume of the combustion chamber, the deformation of the connecting rod increases, but in general does not interfere with the performance of the internal combustion engine. However, when the relative filling of the chamber with liquid exceeds 110-120%, the engine may become inoperable after a hydrolock due to excessive deformation of the connecting rod and jamming of the deformed connecting rod with the piston on the crankshaft at the bottom dead center.

Using modeling, it was also determined that the amount of deformation of the piston pin under overload caused by hydrolock significantly exceeds the permissible clearance of 0,02 mm in the pin-piston interface, with a stress in the middle of the pin close to 700 MPa. This causes a sharp increase in friction in the interface of the pin with the piston and connecting rod, which leads to an increase in the specific pressure on the piston skirt to 7,2 MPa, i.e. more than 2,8 times. In fact, the proposed model makes it possible to objectively evaluate the residual deformation of engine parts, provides a fairly complete and objective picture of the process of deformation and destruction of engine parts during hydrolock, and allows one to explain the complex damage and/or destruction of not only the connecting rod, but also the piston skirt and the piston pin.

The performed modeling of the failure of the internal combustion engine cooling system made it also possible to objectively reproduce the mechanism of the occurrence of a malfunction associated with local thermal damage to the combustion chamber of the engine cylinder in the form of melting of the walls, the appearance of cracks, and loss of valve seats. The time point for the onset of this damage has been established – after 10-20 seconds of engine operation in overheating mode after coolant loss. In this case, the pistons in the cylinders receive minor thermal damage, and the coolant temperature sensors do not have enough time to detect engine overheating and enable the driver to prevent the failure.

In addition, modeling of local thermal damage to the intake valve due to failure of the variable valve timing system using the standard program for calculating the cycle of an internal combustion engine, Lotus Engine Simulation, was carried out. It has been determined that an increase in the temperature of the intake valve head can reach 1000C relative to the operating temperature in full valve opening modes only by reducing the duration of the intake valve timing and lift height. This local temperature increase can lead to thermal deformation (creep) of the valve and engine failure.

Simulation of failure in the lubrication system for typical crankshaft designs shows the continuation of oil supply to the connecting rod bearings for a period of time, which depends on the design and operating mode of the engine and can be up to 10 seconds or more. This allows us to explain the difference in lubrication conditions and the degree of damage to the main and connecting rod bearings in emergency cases of oil supply failure, which is key information for a number of practical cases in determining the cause of failure.

The experimentally established patterns of engine performance failures make it possible to plan the types of engine repair work, optimize spare parts stocks at service enterprises, and reduce vehicle downtime during repairs.

The results of the studies performed, including the developed models, can be used in practice in determining the failure causes of various types of engines, and their use in expert studies can increase the accuracy and objectivity of expert conclusions and reports.



## REFERENCES

To sections 1 and 2

1. Khrulev A., Saraev O. Devising a model of the airflow with dust particles in the intake system of a vehicle's internal combustion engine. *Eastern-European Journal of Enterprise Technologies*, 2021, 2/1 (110), pp. 61–69. DOI: <https://doi.org/10.15587/1729-4061.2021.230113>.
2. Khrulev A.E., Saraiev O.V. *Local Abrasive Wear in Automobile Internal Combustion Engines*. Chisinau: LAP LAMBERT Academic Publishing, 2021. 70 p. ISBN: 978-620-4-72743-1.
3. *Bosch Automotive Handbook*. 9th Edition. Stuttgart, Robert Bosch GmbH, 2014. 1544 p.
4. Donaldson. *Engine Air Filtration for Light, Medium, & Heavy Dust Conditions*. Air Cleaners, Pre-cleaners & Inlet Hoods, Rubber Adapters/Elbows, Filter Indicators, Mounting Bands. Donaldson Company, Inc., 2020. 307 p. Available at: <https://www.donaldson.com/content/dam/donaldson/engine-hydraulics-bulk/catalogs/air-intake/north-america/F110027-ENG/Air-Intake-Systems-Product-Guide.pdf>. 20.04.2023.
5. Stachowiak G.W. *Engineering Tribology*. 3rd ed. / G.W. Stachowiak, A.W. Batchelor, ed. Oxford, Elsevier Butterworth-Heinemann, 2005. 482 p.
6. Ludema K.C. *Friction, wear, lubrication: A textbook in tribology*. Boca Raton, CRC Press, 1996. 261 p.
7. Durst M., Klein G.-M., Moser N. *Automotive Filtration. Basics and examples of air, oil and fuel filtration*. Landsberg/Lech: Verlag modern industrie, 2002. 120 p.
8. Von Durst M., Klein G.M., Moser N. *Filtration in Fahrzeugen: Grundlagen und Beispiele zur Luft-, Öl- und Kraftstofffiltration*. Verlag moderne industrie, Gebundene Ausgabe, 2002. 94 p.
9. Hutten I. *Handbook of Non-Woven Filter Media*. Elsevier Science & Technology Books, 2007. 473 p.
10. MS Motorservice. *Technical Filter Brochure*. MS Motorservice International GmbH, Neuenstadt, 2014. 47 p. Available at: <https://mam.rheinmetall-automotive.com/mc/epaper?guid=14c0224fff44e62c>. 20.04.2023.
11. Trautmann P., Durst M., Pelz A., Moser N. High performance nanofibre coated filter media for engine intake air filtration. *AFS 2005 Conference and Expo*, 2005. 9 p. URL: <https://www.researchgate.net/publication/292649030>.
12. Sutherland K. *Filters and Filtration Handbook*. Oxford, Elsevier Ltd., 2008. 523 p.

13. Filter technical brochure. Service Tips and Info. MSI Motor Service International GmbH, Neckarsulm, 2010. 40 p.
14. Filters. Catalogue. MS Motor Service Neuenstadt, MS Motor Service International GmbH, 2014. 1012 p.
15. Perlmutter B. Solid-Liquid Filtration: Practical Guides in Chemical Engineering. Oxford, Butterworth-Heinemann, 2015. 136 p.
16. Dziubak T., Dziubak S.D. Experimental Study of Filtration Materials Used in the Car Air Intake. *Materials*, 2020, 13, 3498. 20 p. DOI: <http://doi.org/10.3390/ma13163498>.
17. Perlmutter B. Solid-Liquid Filtration: Practical Guides in Chemical Engineering. Oxford, Butterworth-Heinemann, 2015. 136 p.
18. Ferguson C.R., Kirkpatrick A.T. Internal Combustion Engines. Third Edition. Chichester, John Wiley & Sons, Ltd., 2016. 460 p.
19. Hoag K., Dondlinger B. Vehicular Engine Design. 2d Edition. Vienna, Springer Vienna, 2016. 386 p.
20. Lakshminarayanan P.A., Nayak N.S. Critical component wear in heavy duty engines. John Wiley & Sons (Asia) Pte Ltd., 2011. 424 p.
21. Van Basshuysen R. Internal Combustion Engine. Basics, Components, Systems, and Perspectives / R. Van Basshuysen, F. Schäfer. Warrendale, SAE International, 2004. 812 p.
22. Yamagata H. The science and technology of materials in automotive engines, Woodhead Publishing Limited, Cambridge, England, 2005. 318 p.
23. Rahnejat H. Tribology and Dynamics of Engine and Powertrain: Fundamentals, Applications and Future Trends. Woodhead Publishing, 2010. 1018 p.
24. Almeida A.L., Azevedo E.V., Yoshino F.J., Oliveira M.J., Trindade W.R. Increase of engine air filter elements service interval for medium and heavy duty vehicles by means of air induction system design optimization. XXV Simpósio Internacional de EngenhariaAutomotiva, 2017. 9 p. DOI: <http://doi.org/10.5151/engpro-simea2017-30>.
25. Zhang P., Duan J., Chen G., Wang W. Numerical Investigation on Gas-solid Flow in a Circumfluent Cyclone Separator. *Aerosol Physics and Instrumentation*, 2019, 19, 5, pp. 971–980. DOI: <http://doi.org/10.4209/aaqr.2018.05.0197>.
26. Tang Z., Yu L., Wang F., Li N., Chang L., Cui N. Effect of Particle Size and Shape on Separation in a Hydrocyclone. *Water*, 2019, 11, 16, 19 p. DOI: <http://doi.org/10.3390/w11010016>.
27. Pulkrabek W.W. Engineering Fundamentals of the Internal Combustion Engine. New Jersey, Prentice Hall, 1997. 411 p.

28. Dziubak, T. Operational properties of performance engine intake air cleaners. *Combustion Engines*, 2018, 172(1), pp. 25-34. DOI: <https://doi.org/10.19206/CE-2018-103>
29. Han S., Kim J., Ko S.H. Advances in air filtration technologies: structure-based and interaction-based approaches. *Materials Today Advances*, 2021, 9(4). 13 p. DOI: <http://doi.org/10.1016/j.mtadv.2021.100134>.
30. King R.P. *Modeling and Simulation of Mineral Processing Systems*. Butterworth-Heinemann, Woburn, 2001. 403 p.
31. Malmborg P. Engine air filters requirements. How different running conditions affect service life. Karlstad, Karlstads Universitet, 2019. 40 p.
32. Sukhapure K., Burns A., Mahmud T., Spooner J. CFD Modelling and Validation of Head Losses in Pipe Bifurcations. Slovenia, 13th International Conference on Heat Transfer, Fluid Mechanics and Thermodynamics, 2017, pp. 489–494.
33. Matoušek V. *Flow Mechanism of Sand-Water Mixtures*. Delft, Delft University Press, 1997. 258 p.
34. Rudinger G. *Fundamentals of Gas Particle Flow*. Elsevier, 2012. 156 p.
35. Khrulev A. Internal combustion engines: Fault expertise and analysis. In 2 vol. V.2. Practical determination of fault causes. Chisinau, LAP LAMBERT Academic Publishing, 2023. 562 p. ISBN: 978-620-6-15367-2.
36. ANSYS Free Student Software Downloads. ANSYS, Inc., 2019. Available at: <https://www.ansys.com/academic/free-student-products>. 20.10.2019.
37. ANSYS. *Theory Reference. Release 5.6 / Edited by Peter Kohnke, Ph.D.* ANSYS Inc., Canonsburg, PA 15317, 1999. 1286 p.
38. Rebollo T.Ch., Lewandowski R. *Mathematical and Numerical Foundations of Turbulence Models and Applications*. Springer, 2014. 517 p.
39. Isermann, R. *Combustion Engine Diagnosis: Model-based Condition Monitoring of Gasoline and Diesel Engines and their Components*. Springer-Verlag, 2017. 303 p.

To section 3

40. Khrulev A. Method of compiling and using the vehicles history at their technical condition study in the tasks in determining the failure causes of the units and assemblies. *Criminalistics and Forensics*, 2020, Vol. 65, pp. 594-605. DOI: <https://doi.org/10.33994/kndise.2020.65.59>.
41. Khrulev A., Dmitriev S. Study of the conrod deformation during piston interaction with liquid in the internal combustion engine cylinder. *Journal of Mechanical*

Engineering and Sciences, 2019. Volume 14, Issue 2, pp. 6557-6569. DOI: <https://doi.org/10.15282/jmes.14.2.2020.03.0515>.

42. Dubey A.M., Mohta L.A. Design and Analysis of Connecting Rod with Mass Optimization. *International Journal for Scientific Research & Development*, 2017. 4 (11), pp. 548-552.

43. Nagaraju K.L., Chandan R. Buckling Analysis of Connecting Rod. *International Research Journal of Engineering and Technology*, 2016. 03(08), pp. 1358–1361.

44. Greuter, E., Zima, S. Engine Failure Analysis. *Internal Combustion Engine Failures and Their Causes*. SAE International, 2012. 582 p.

45. Khrulev A. Internal combustion engines: Fault expertise and analysis. In 2 vol. V.1. *Methods and means of expert research*. Chisinau, LAP LAMBERT Academic Publishing, 2023. 429 p. ISBN: 978-620-6-15137-1.

46. Strozzi A., Baldini A., Giacopini M., et al. A repertoire of failures in connecting rods for internal combustion engines, and indications on traditional and advanced design methods. *Engineering Failure Analysis*, 2016. Vol. 60, pp. 20-39. DOI: <http://dx.doi.org/10.1016/j.engfailanal.2015.11.034>.

47. Khrulev A.E. Simulation of the connecting rod damage when fluid enters the engine cylinder. *Vehicle and Electronics. Innovative Technologies*, 2020, 17, pp. 5-18. DOI: <http://dx.doi.org/10.30977/VEIT.2226-9266.2020.17.0.5>.

48. *Engine Failure Analysis and Tips Job Aid. Guide to Preventing Repeat Engine Failures*. Version 1.0. Detroit, FORD Motor Company, 2013. 24 p.

49. Kumar P.S., Kumar K. Buckling Analysis and Shape Optimization of Connecting Rod using FEA. *REST Journal on Emerging trends in Modelling and Manufacturing*, 2016. 2(2), pp. 44–50.

50. Shenoy P.S., Fatemi A. Dynamic analysis of loads and stresses in connecting rods. *J.Mechanical Engineering Science. Proc.IMEchE*. 2006, 220(C), pp. 615–624. DOI: <https://doi.org/10.1243/09544062JMES105>.

51. Bedse D.S. Design Evaluation of Connecting Rod. *International Journal of Recent Engineering Research and Development*, 2017, 02 (07), pp. 203-213.

52. Khrulev A.E., Dmitriev S.A. Some aspects of influence of the connecting rod design on the output parameters of high-speed internal combustion engines. *Problems of Friction and Wear*, 2020, №1(86), pp. 23-37. DOI: [https://doi.org/10.18372/0370-2197.1\(86\).144855](https://doi.org/10.18372/0370-2197.1(86).144855).

53. Frățița M., Uzuneanu K., Balanescu D.T. About I-beam versus H-beam connecting rod design using Inventor Autodesk 2018. *The 8th International Conference on Advanced Concepts in Mechanical Engineering, IOP Conference Series: Materials Science*

and Engineering, 2018, 444 (072008). 8 p. DOI: <https://doi.org/10.1088/1757-899X/444/7/072008>.

54. Gunjal N.U., Shinde V.B. Analysis of Connecting rod using Reverse Engineering method and modify the design using polynomial curve. *International Journal of Advance Research and Innovative Ideas in Education*, 2016, 2 (4), pp. 467-474.

55. Haider A.A., Kumar A., Chowdhury A., Khan M., Suresh P. Design and Structural Analysis of Connecting Rod. *International Research Journal of Engineering and Technology*, 2018, 05(05), pp. 282–285.

56. Jayaprakash V., Rohit A.K., Srinivas Ch. Non Linear Analysis of Diesel Engine Connecting Rod. *International Journal of Trend in Scientific Research and Development*, 2018, 2 (6), pp. 478–488.

57. Manda M., Kola R., Karunakarreddy K. Modal Analysis of a Connecting Rod using ANSYS. *International Journal of Mechanical Engineering*, 2017, 4 (4), pp. 30-35.

58. Mohammed M.N., Omar M.Z., Sajuri Z. Failure Analysis of a Fractured Connecting Rod. *Journal of Asian Scientific Research*, 2011, V.2, pp. 737–741.

59. Mohankumar D., Rakesh L. Design and Analysis of a Connecting Rod. *International Journal of Pure and Applied Mathematics*, 2017, 116 (15), pp. 105-108.

60. Nagaraju K.L., Chandan R. Buckling Analysis of Connecting Rod. *International Research Journal of Engineering and Technology*, 2016, 03(08), pp. 1358–1361.

61. Shenoy P.S. *Dynamic Load Analysis and Optimization of Connecting Rod*. Toledo, University of Toledo, 2004, 188 p.

62. Magdas V.B., Mastan D. C., Burnete N. Simulation possibilities of the internal combustion engine management elements using Lotus Engine Simulation software. *IOP Conf. Series: Materials Science and Engineering*, 2020, 997. 11 p. DOI: <https://doi.org/10.1088/1757-899X/997/1/012121>.

63. Magopets S.O., Krasota M.V., Bevs O.V., Shepelenko I.V., Matvienko O.O. *Automobile engines. Thermal, kinematic and dynamic calculation of the engine using the MathCAD program*. Kirovohrad, KNTU, 2014. 82 p.

64. Dyachenko V.G. *Internal combustion engines. Theory* / Edited by A.P. Marchenko. Kharkiv, NTU KhPI, 2008. 488 p.

65. Ganesan V. *IC Engines*. Fourth Edition. New Delhi, Tata McGraw Hill Education Private Limited, 2012. 730 p.

66. Heywood J.B. *Internal Combustion Engine Fundamentals* (McGraw–Hill Series in Mech. Engineering). New York, McGraw–Hill, Inc., 1988. 930 p.

67. Shapko V.F. Automobile engines. Fundamentals of the theory and characteristics of internal combustion piston engines: a study guide. Kharkiv, Tochka, 2014. 148 p.
68. Haschuk P.M., Nikipchuk S.V. Modeling of heat exchange processes occurring in the cylinders of an internal combustion engine. *Fire Safety*, 2018, No. 33, pp. 15-34. DOI: <https://doi.org/10.32447/20786662.33.2018.03>.
69. Levterov A.M., Levterova L.I. Analysis of mathematical models of the mechanism of soot formation during the combustion of hydrocarbon fuels. *Bulletin NTU KhPI. Series: Mathematical modeling in engineering and technology*, 2013, No. 5 (979), pp. 130–141.
70. Duleba B. Simulation of Automotive Engine in Lotus Simulation Tools. *Transfer inovacii*, 2014, No. 30, pp. 48-52.
71. Lotus Engineering Software (LESOFT). Group Lotus PLC, 2019. Available at: <http://www.lesoft.co>. 20.10.2021.
72. Kumar R., Saxsena N., Singh A. Finite Element Analysis of Connecting rod for Internal Combustion Engines: A Review. *International Research Journal of Engineering and Technology*, 2017, 04(02), pp. 1699–1702.
73. Gere J.M. *Mechanics of Materials*. 6th Edition. Belmont, Brooks/Cole – Thomson Learning, 2004. 940 p.
74. Pisarenko G.S., Kvitka O.L., Umansky E.S. *Resistance of materials*. 2nd ed. /under the editorship H.S. Pysarenko. Kyiv, Vyshcha Shk., 2004. 655 p.
75. Lemonis M.E. Moments of Inertia. Reference Table. *Calculation Tools & Engineering Resources*, 2020. Available at: <https://calcresource.com/moments-of-inertia-table.html>. 17.11.2021.
76. Kosenko V.A., Kushchevska N.F., Dobrovolskyi O.H., Malyshev V.V. *Materials and materials science in automobile transport*. Kyiv, "Ukraine" University, 2015. 314 p.
77. Marchenko A.P., Ryazantsev M.K., Shekhovtsov A.F. *Internal combustion engines. T.1. Development of structures of forced engines of ground transport vehicles / Edited by Prof. A.P. Marchenko, Prof. A.F. Shekhovtsov*. Kharkiv, Publishing House Center of NTU KhPI, 2004. 491 p.
78. MAHLE. *Piston and Engine Testing*. Stuttgart, Vieweg Teubner Verlag, Springer Fachmedien Wiesbaden GmbH, 2012. 284 p.
79. Khrulev A.E., Dmitriev S.O. Calculation model of the process of compression of air with a liquid in the cylinder of an internal combustion engine. *Bulletin of the National Transport University. Series Technical Sciences*, 2020, No. 1 (46), pp. 416-426. DOI: <https://doi.org/10.33744/2308-6645-2020-1-46-416-426>.

80. Zhiwei Yu., Xiaolei X., Hongxin D. Failure analysis of a diesel engine piston-pin. *Engineering Failure Analysis*, 2007, 14(1), pp. 110-117. DOI: <http://doi.org/10.1016/j.engfailanal.2005.12.004>.

81. Khrulev A., Sarayev O. Building a mathematical model of the destruction of a connecting rod-piston group in the car engine at hydraulic lock. *Eastern-European Journal of Enterprise Technologies*, 2022, 3/7 (117), pp. 40-49. DOI: <https://doi.org/10.15587/1729-4061.2022.259454>.

82. Abu-Nada E., Al-Hinti I., Al-Sarkhi A., Akash B. Effect of Piston Friction on the Performance of SI Engine: A New Thermodynamic Approach. *Journal of Engineering for Gas Turbines and Power*, 2008, 130 (2), pp. 1-8. DOI: <https://doi.org/10.1115/1.2795777>.

83. Kozuba J., Wieszała R., Mendala J., Roszak M., Pakieła W. Selected tribological parameters for silumin alloy used for engine piston. *Archives of Materials Science and Engineering*, 2021, Vol.107, Issue 2, pp. 64-71. DOI: <https://doi.org/10.5604/01.3001.0015.0243>.

84. Petko I.V., Bondarenko M.Y., Kostrytskyi V.V. Calculation and design of electromechanical devices. Kyiv, KNUTD, 2016. 328 p.

85. Gerasymchuk O.M. Calculation and selection of landings with tension. Electronic bulk edition. Kyiv, Polytechnic, 2010. 26 p.

86. Khrulev O.E., Dmitriev S.O. Some aspects of increasing the initial parameters of the internal combustion engine during modernization in the conditions of serial production. *Internal combustion engines*, 2019, No. 1, pp. 63-72. DOI: <https://doi.org/10.20998/0419-8719.2019.1.10>.

87. Alawadhi E.M. Finite Element Simulations Using ANSYS. Boca Raton, CRC Press, 2010. 416 p.

88. Thakur S.S., Patil G. Harmonic Analysis of Connecting rod using ANSYS. *International Journal for Science and Advance Research in Technology*, 2017, 3 (1), pp. 104-110.

89. Khrulev A.E., Kochurenko Yu.V. Methodology for determining the cause of internal combustion engine malfunctions in case of severe operational damage. *Internal combustion engines*, 2017, No. 1, pp. 52-60. DOI: <https://doi.org/10.20998/0419-8719.2017.1.10>.

To section 4

90. Khrulev A.E., Saraev O.V. The method of expert assessment of the technical condition of an automobile engine after overheating. *Automobile Transport*, 2021, 48, pp. 5-16. DOI: <https://doi.org/10.30977/AT.2219-8342.2021.48.0.5>.

91. Khrulev A.E., Sarayeva I.Yu., Vorobyov O.M., Sokhin A.A. Assessment of the possibility of using mathematical models for expert studies of car engine damage. *Automobile and electronics. Modern technology*, 2022, No. 21, pp. 79–86. DOI: <https://doi.org/10.30977/VEIT.2022.21.0.06>.

92. Khrulev A., Dmitriev S. Thermal Damage to Intake Valves in ICE with Variable Timing. *International Journal of Automotive and Mechanical Engineering*, 2019, Vol. 16, Issue 4, pp. 7243–7258. DOI: <https://doi.org/10.15282/ijame.16.4.2019.06.0540>.

93. Audi 2.8l and 3.2l FSI engines with Audi valvelift system. Self-Study Programme 411. Ingolstadt, AUDI AG, 2007. 63 p.

94. Vehicle cooling. A compact guide for the workshop. Stuttgart, MAHLE Aftermarket GmbH, 2012. 76 p.

95. Cooling Systems. Application & Installation Guide. LEBW4978-16 (11-17). Irving, Caterpillar, 2017. 128 p.

96. Mancarella A., Marello O. Effect of Coolant Temperature on Performance and Emissions of a Compression Ignition Engine Running on Conventional Diesel and Hydrotreated Vegetable Oil (HVO). *MDPI, Energies*, 2023, Vol. 16, 144. 27 p. DOI: <https://doi.org/10.3390/en16010144>.

97. Jack T.K., Ojapah M.M. Water-Cooled Petrol Engines: A Review of Considerations in Cooling Systems Calculations with Variable Coolant Density and Specific Heat. *International Journal of Advances in Engineering & Technology*, 2013, 6 (2), pp. 659–667. Available at: <https://www.researchgate.net/publication/329179166.27.03.2020>.

98. Missan G.S., Keswani I.P. Analysis of Causes of Engine Overheating due to Cooling System Failure Using Pareto Principle. *International Journal of Engineering Trends and Technology (IJETT)*, 2016, Vol.36, No. 5, pp. 242–248.

99. Naga Prasad C.S. Thermal Analysis of Engine Failure Conditions in Engine Overheating Cases. *International Journal of Research*, 2017, 4 (17), pp. 4020–4025. Available at: <https://journals.pen2print.org/index.php/ijr/article/view/11396/10849.27.03.2020>.

100. Prudhvi G., Vinay G., Suresh Babu G. Cooling Systems in Automobiles and Cars. *International Journal of Engineering and Advanced Technology*, 2013, 2 (4), pp. 688–695. Available at: <http://citeseerx.ist.psu.edu/viewdoc/download?doi=10.1.1.675.706&rep=rep1&type=pdf>. – 27.03.2020.

101. Janna, W.S. *Engineering Heat Transfer*. New York, CRC Press, 2009. 692 p.

102. Incropera F.P., DeWitt D.P., Bergman T.L., Lavine A.S. *Fundamentals of Heat and Mass Transfer*. 6-th Edition. John Wiley & Sons, Inc., 2007. 1071 p.

103. Chiodi M. An Innovative 3D–CFD Approach towards Virtual Development of Internal Combustion Engines. Wiesbaden, Vieweg+Teubner Verlag / Springer Fachmedien, 2011. 245 p.
104. Yadav R., Sanjay B.E. Thermodynamics & Heat Engines. Allahabad: Central Publishing House, 2001. 746 p.
105. Wang C.S., Berry G.F. Heat Transfer in Internal Combustion Engines. New York, The American Society of Mechanical Engineers, 10017 85–WA/HT–23, 2017, pp. 1–7.
106. Ziong N.V., Belogub A. The method of forecasting temperature and stress fields of the internal combustion engine piston. Transport systems and means. Problems of operation and diagnostics: monograph. Kherson, KhDMA, 2019, pp.9-27.
107. MAHLE. Cylinder components. Stuttgart, Vieweg Teubner Verlag, Springer Fachmedien Wiesbaden GmbH, 2010. 130 p.
108. Reconditioning of Aluminium Engine Blocks. Service Tips & Information. Neckarsulm, MSI Motor Service International GmbH, 2006. 100 p.
109. Lewis R., Dwyer-Joyce R.S. Automotive Engine Valve Recession. London, Professional Engineering Publishing Limited, 2002. 138 p.
110. Engine Bearing Failure Analysis Program. Mahle-Clevite. Stuttgart: MahleGmbH, 2022. Available at: <https://www.mahle-aftermarket.com/na/en/support/clevite-engine-bearing-failure-analysis/>. 16.12.2022.
111. Valve damage and causes. TRW / MSI Motor Service, KSPG Automotive Group, 50 003 976–09, 2010. 4 p.
112. Azadi M., Roozban M., Mafi A. Failure analysis of an intake valve in a gasoline engine. The Journal of Engine Research, 2012, Vol.26, pp. 03–09.
113. Morehouse D., Porter J., Hiltz J. and Brauss M. Diesel Engine valve failures. NOR 1L0, B2Y 3Z7. Ontario, Defence Research Development Canada Atlantic, 2004. 15 p.
114. Raghuvanshi N.Kr., Pandey A., Mandloi R.K. Failure Analysis of Internal Combustion Engine Valves: A Review. International Journal of Innovative Research in Science, Engineering and Technology, 2012, Vol. 1, Issue 2, pp. 173–181.
115. Khrulev A.E., Dmitriev S.O. Features of modeling the temperature state of the intake valves of internal combustion engines in the tasks of finding the fault causes. Problems of friction and wear, 2019, No. 1 (82), pp. 39-51. DOI: [https://doi.org/10.18372/0370-2197.1\(82\).13485](https://doi.org/10.18372/0370-2197.1(82).13485).
116. Zhang Q., Zuo Z., Liu J. Failure analysis of a diesel engine cylinder head based on finite element method. Engineering Failure Analysis, 2013, 34, pp. 51-58. DOI: <http://doi.org/10.1016/j.engfailanal.2013.07.023>.

117. Wishniewsky T.S., Furmansky P. Thermal Contact Conductance of Valve Face/Seat Interface in IC Engine. Conductivity 24. Joint Conference. Pittsburg, 1999, pp.97-104.

118. Iliev S. Heat transfer investigation in the intake port of four stroke direct injection compression ignition engine. Acta Technica Corviniensis, Bulletin of Engineering, 2013, No.1, pp. 133-138. DOI: <https://doi.org/10.13140/2.1.3947.5847>.

119. ISO 683-15:1992. Heat-treatable steels, alloy steels and free-cutting steels. Part 15: Valve steels for internal combustion engines. ISO/TC 17/SC 4, 1992. 11 p.

To section 5

120. Moon S.M., Cho Y.J., Kim T.W. Evaluation of lubrication performance of crank pin bearing in a marine diesel engine. Friction, 2018, 6(4), pp. 464–471. DOI: <https://doi.org/10.1007/s40544-017-0196-0>.

121. Sun J., Li B., Zhu S., Miao E., Wang H., Zhao X. & Teng Q. Lubrication Performance of Connecting-Rod and Main Bearing in Different Engine Operating Conditions. Chinese Journal of Mechanical Engineering, 2019, Vol.32, No.23. 12 p. DOI: <https://doi.org/10.1186/s10033-019-0335-9>.

122. Plain Bearings. Spherical plain bearings. Rod ends. Plain bushes. Thrust washers, strips. Schweinfurt: Schaeffler Technologies AG & Co. KG, 2016. 438 p.

123. Kopeliovich D. Engine bearing failures and how to avoid them. King Bearings. Available at: <https://www.kingbearings.com/wp-content/uploads/2014/10/Engine-bearing-failures-and-how-to-avoid-them1.pdf> 18.10.2021.

124. Laguna-Camacho J.R., Sánchez-Yáñez S.M., Juárez-Morales G. et al. A Wear Analysis Carried On Connecting Rod Bearings From Internal Combustion Engines. Engineering Failure Analysis, 2020. 16 p. DOI: <http://dx.doi.org/10.5772/intechopen.89263>.

125. Damage to engine bearings. Knowledgepool. Neuenstadt, MS Motorservice International GmbH, 2017. 71 c.

126. Engine Bearings. Failure & Analysis Guide. Clevite Issue. Ann Arbor, Mahle Clevite Inc., 2008. 32 p.

127. Engine Bearings. Failure & Analysis Guide. Clevite 77, Form # CL77–3–402 1350. Ann Arbor, Dana Corporation, 2008. 32 p.

128. Engine Bearings: Failure Analysis and Correction. Farmington Hills, MAHLE Aftermarket Inc., 2014. 39 p.

129. Engine Bearing Failure Analysis Guide. A guide to analysis and correction of premature engine bearing failures. Form # CEB-1-1208. Ann Arbor, Mahle Clevite Inc., 2008. 26 p.

130. Premature Failures Manual. São Paulo, MAHLE Metal Leve S.A., 2014. 68 p.

131. Khrulev O.E., Saraev O.V., Sarayeva I.Yu. The influence of centrifugal forces on the lubrication of crankshaft bearings in emergency modes operation of the car engine. Bulletin of Machine Building and Transport, 2021, Volume 12, Issue 2, pp. 112-121. DOI: <https://doi.org/10.31649/2413-4503-2020-12-2-112-121>.

132. Naffin R.K., Chang L. An Analytical Model for the Basic Design Calculations of Journal Bearings. Journal of Tribology, 2010, Vol.132. 7 p. DOI: <https://doi.org/10.1115/1.4000941>.

133. Idelchik I.E. Handbook of Hydraulic Resistance. Coefficients of Local Resistance and of Friction. New York, Israel Program for Scientific Translations Ltd., 1966. 517 p.

To section 6

134. Technical operation of road transport. Under. ed. M. N. Bednyaka. Kiev, 1979. 295 p.

135. Govorushchenko N. Ya. Technical operation of automobiles. Charkov, 1984. 312 p.

136. Gillespie Thomas D., 1992.: Fundamentals of Vehicle Dynamics. Society of Automotive Engineers, Inc. – 470 p.

137. Lobas L.G., Verbitsky V.G. Qualitative and analytical methods in the dynamics of wheeled vehicles. Kiev, 1990. 232 p.

138. Bazhinov O.V., Kravchenko O.P. Reliability of the semi-trailer truck. Monograph. Lugansk, V. Dahl East-Ukraine National University, 2009. 456 p.

139. Kravchenko O., Veritelnik E. Analysis of the operational reliability of VOLVO FH 1242 tractor-trailers. Scientific notes. № 36, Luck, 2012, pp. 165 – 168.

140. Kravchenko O., Veritelnik E. Study of malfunctions of VOLVO FH 1242 tractor-trailers during the warranty and post-warranty periods of operation. Bulletin of SevNTU: Collection of scientific papers. Series of Mechanical Engineering and Transport, issue 142/2013, Sevastopol: SevNTU, 2013, pp. 100 – 103.

141. Kravchenko O., Veritelnik E. Study of malfunctions of tractor-trailer vehicles during warranty and post-warranty periods of operation. Bulletin of the KhPI National

Technical University, No. 29(1002), KhPI National Technical University, Kharkiv, 2013, pp. 106 – 113.

142. Kravchenko O. Analysis of operational reliability of diesel engines of Mercedes-Benz 1844 ACTROS LS tractor units. Modern technologies in mechanical engineering and transport. Scientific journal. №1(5). Lutsk: LNTU, 2016. pp. 83-87.

143. Kravchenko O., Veritelnik E. Monitoring the consumption of spare parts for VOLVO FH 1242 tractor-trailers. Bulletin of the KhPI National Technical University, №. 9(1052), KhPI National Technical University. Kharkiv, 2014, p. 33-37.

144. Kravchenko O., Veritelnik E. Reducing of car repair's downtime by optimizing of spare parts warehouse for freight transport companies. Scientific notes. Interuniversity collection (by fields of knowledge "Mechanical engineering and metalworking", "Engineering Mechanics", "Metallurgy and metallurgy"), № 46, Luck, 2014, pp. 301-306.

145. Kravchenko O., Veritelnik E. Development criterion the necessity of details storing or not storing on autoenterprise. Volodymyr Dahl Bulletin of the Eastern Ukrainian National University named after. №2(219), 2015., p. 77-82.

146. S. Chan Choi, Wayne S. Desarbo, Patrick T. Harker, "Product positioning under price competition", *Management Science* 36(2), pp. 175–199 (1990).

147. T. J Brignall, L. Fitzgerald, R. Johnston, R. Siverstro, "Product costing in service organizations", *Management Accounting Research* 2(4), pp. 227–248 (1991).

148. K. de Ruyter, M. Wetzels, J. Bloemer, "On the relationship between perceived service quality, service loyalty and switching costs", *International Journal of Service Industry Management* 9(5), pp. 436–453 (1998).

149. A. Gunasekaran, "Just-in-time purchasing: An investigation for research and applications", *International Journal of Production Economics* 59(1-3), pp. 77–84 (1999).

150. S. Ray, S. Li, Y. Song, "Tailored supply chain decision making under price-sensitive stochastic demand and delivery uncertainty", *Management Science* 51(12), pp. 1733–1902 (2005).

prof. Olexandr Kravchenko, Dr. Sc. Tech.  
senior researcher Ing. Alexander Khrulev, Dr. Sc. Tech.  
prof. Dr. Ing. Juraj Gerlici, prof. h. c.  
prof. Oleksii Saraiev, Dr. Sc. Tech.

**MODELING OF LOCAL DAMAGE  
IN AUTOMOBILE INTERNAL COMBUSTION ENGINES**

Copyright©University of Žilina, 2025  
Printed by EDIS Publishing House UNIZA, Univerzitná HB, 010 26 Žilina  
First edition  
Number of copies 50, AA 14 92  
ISBN 978-80-544-2239-8  
[www.edis.unisa.sk](http://www.edis.unisa.sk)  
[edis@unisa.sk](mailto:edis@unisa.sk)



The monograph examines a number of hitherto unnoticed and insufficiently studied mechanisms of failure that cause local operational damage in automobile internal combustion engines. The general concept of modeling processes and mechanisms of the origin and development of engine failures is presented. The task, possibilities, purpose and features of mathematical modeling of processes that lead to damage and failure of engines are determined. The difference between modeling of operational engine damage and modeling during design and research work is shown. The main processes of local damage in engines are considered, mathematical models of the considered processes are described in detail, and the results of modeling on examples of specific structures are presented. Based on the research results, it was concluded that the developed models can be used in practice in identifying the causes of engine failures of various types, and their use in professional studies can increase the accuracy and objectivity of expert opinions. The book is intended for undergraduate, graduate and postgraduate students, as well as researchers in the field of Automotive Operation, but may also be useful for engineers, professionals and scientists in other fields related to process research, design and operation of internal combustion engines.

[www.edis.uniza.sk](http://www.edis.uniza.sk)



9 788055 422398